University Library

A gateway to Melbourne's research publications

Minerva Access is the Institutional Repository of The University of Melbourne

Author/s:
Swami, G;Thai, H-T;Liu, X

Title:
Structural robustness of composite modular buildings: The roles of CFST columns and inter-module connections

Date:
2023-02-01

Citation:
Swami, G., Thai, H. -T. & Liu, X. (2023). Structural robustness of composite modular buildings: The roles of CFST columns and inter-module connections. Structures, 48, pp.1491-1504. https://doi.org/10.1016/j.istruc.2023.01.052.

Persistent Link:
https://hdl.handle.net/11343/332577

Structural robustness of composite modular buildings: The roles of CFST columns and inter-module connections

Gaurav Swami, Huu-Tai Thai*, Xuemei Liu

Department of Infrastructure Engineering, The University of Melbourne, Parkville, VIC, Australia

Abstract

This paper explores the important roles of concrete filled steel tube (CFST) columns and inter-module connections on the structural robustness of composite modular buildings. Various numerical models were developed for concrete filled steel tube (CFST) columns, semi-rigid frames, and conventional steel buildings under column removal scenarios to verify the validation of the present study. A numerical model of a 10-storey composite modular building was then developed, in which conventional hollow steel section columns were replaced by CFST columns to improve resistance against buckling of columns. To examine the behavior and force transmission mechanism of composite modular buildings under various module removal situations, nonlinear dynamic and nonlinear static pushover analyses was conducted. The introduction of CFST columns provided resistance against buckling of columns under high axial forces. It was observed that a pin-joint inter-module connection approach is a conservative approach to model the connections between modules. It was discovered that the dynamic amplification factor (DAF) recommended by the general service administration (GSA) for the nonlinear static analysis overestimates the displacement response of the modular building structure under module loss situations. The modular building was deemed safe against progressive collapse without excessive failure of the component members. However, progressive failure of the modular building under corner module removal scenario was observed in pushover analysis due to shear failure of horizontal inter-module connections. It

* Corresponding author. Tel.: +61 3 8344 6196
E-mail address: tai.thai@unimelb.edu.au (H.T. Thai)

was observed that the corner module removal scenario is more critical as compared to the column removal scenario for modular buildings. Based on the location of module removal, the DAF values of 1.65 and 1.2 were recommended for corner module removal and internal and edge module removal, respectively.

Keywords: Modular building; progressive collapse; CFST column; semi-rigid joint

1. Introduction

Modular buildings are composed of components produced on assembly lines in industrial units and then assembled on site in a desired configuration. The construction process includes manufacturing of modular units in a factory-controlled environment, transportation to the site, and quick assembly at site to form the entire building [1]. Due to the higher number of repeated modules, especially for tall structures, this approach offers several advantages over traditional on-site construction, including time and money savings, superior quality control, increased productivity, and reduced construction waste. Higher quality control is achieved for modular buildings as the modules are fabricated in a factory-controlled system. Assembly of modules with suitable inter-module connections is the primary work to be executed on-site. The primary load path for the transfer of forces between modules is made up of the inter-module connections.

Multi-story structures are severely impacted by incidents like fire, blast, explosion, and collision, especially when the primary load-bearing components are compromised. If there are no other available alternative load paths, the initial local failure can cause the primary load path to break, which could then result in progressive collapse [2]. Following the Ronan Point collapse in 1968 as shown in Fig. 1, substantial research on the progressive failure and structural robustness of traditional buildings was carried out, and design specifications were also established [3]. The progressive collapse analysis became increasingly important for

building design, especially after explosive attacks to essential buildings such as World Trade Center in New York as shown in Fig. 1 [3].

Since modular building is such a new kind of construction in terms of research and industrial practices, this potential destructive collapse behavior in modular construction has not been well addressed. The recent developments in the field of modular construction involves construction of multi-storey buildings as steel-framed structures [4, 5]. However, the drawbacks of steel, such as low buckling strength, corrosion, low thermal resistance, etc. calls for an advancement of composite material of steel and concrete. Composite members such as the CFST columns have manifold advantages over steel columns such as improved fire resistance, increased concrete compression strength due to the confinement effect by steel tube, delayed local buckling due to the interaction between concrete and steel tube [6]. CFST columns also allow a structural designer to reduce the effective column section sizes, thereby providing more open area in a limited size module. There has been limited research on the dynamic behavior of modular buildings observed due to the sudden loss of structural elements after accidental events of fire, blast, earthquake, etc leading to progressive failure of the entire structure. Many of such studies have only considered analysis within design parameters, taking into account steel framed structures with either rigid or pinned connections, which can cause an overestimation or underestimation of the capacity of such structures [4, 5, 7-9].

Researchers and engineers have been paying more attention to the modular construction in recent years. Extensive state-of-the-art literature studies on the structural performance of modular structures and the design of inter-module connections have been done in Refs. [10-14]. Typically, inter-module connections and individual structural elements are investigated using experimental programs, and their outcomes are verified using analytical and numerical research [13, 15, 16]. While the only approach that can be used to investigate how multi-story modular structures function under wind, earthquake, abnormal loading, and progressive

collapse is numerical simulation using the FE method [4, 5, 7-9, 17, 18]. With a reasonable material model and effective modelling technique, the FE method has emerged as the primary analysis tool for predicting the behavior of steel-concrete composite multi-storey buildings under severe events.

The various modelling techniques are divided into two categories “shell-solid” models and “beam-shell” models [19-22]. The concrete slab is modelled by solid components in the shell-solid model, whereas the steel beam is modelled by shell elements. [19, 20]. Whereas, the beam-shell model employs multilayer shell elements for the concrete slab and beam elements for steel beams. [21]. For predicting the structural response of steel-concrete composite multi-story structures, it has been found that both models have good precision, but the beam-shell model has a greater computing efficiency and a faster modelling speed [19-22].

Fu [5] studied the progressive failure response of a 20-storey conventional steel-framed building with concrete slabs in ABAQUS software. The dynamic response of the structure was determined to be mostly linked to the affected loading area following column removal, which also determines the amount of energy required to be absorbed by the building. It was also discovered that removing columns at a higher elevation induced higher vertical displacements than removing columns at the ground level [5, 23]. Luo et al. [4] observed that the collapse resistance of steel modular buildings could be enhanced with higher number of modules in a floor, higher buckling strength of supporting posts, the use of longitudinal wall bracing and higher rotational stiffness of inter-module joints. Due to the slab-related contact interaction and diaphragm action, consideration of floor slabs provided a more realistic description of collapse mechanisms [4]. Alembagheri et al. [15] studied the progressive failure response of typical modular steel building with rigid modules. It was observed that collapse in the rigid-module modular building is generally induced by the shear failure of horizontal connections, connecting the modules in the damaged bays to the adjacent bays. It was also concluded that

pinned connections can be sufficient to achieve acceptable robustness under the extreme condition of gravity-induced progressive collapse scenarios on a rigid-module modular building [15, 24].

According to Thai et al. [9], inter-module connections and lateral bracing systems in the modular units both contribute significantly to the robustness of the 12-story modular structures. Additionally, it was determined that the loss of the corner member is the most crucial scenario since there are not many adjacent members to properly distribute the loads. The progressive collapse of a high-rise modular structure was examined by Chua et al. [18] using nonlinear static analysis and a proposed pin-ended joint model under the scenario of column removal using solid elements. In the study, a DAF value of 2.0 was used to account for the dynamic effect. However, no dynamic analysis was conducted, therefore it is uncertain whether a DAF of 2.0 is sufficient for the robustness design of the steel modular construction [18]. In most cases, the gradual collapse of a modular structure has been attributed to the buckling of nearby columns or to the insufficient capacity of horizontal inter-module connections to transfer loads in the event of module or column removal scenarios [4, 7, 9, 17, 18].

From a structural viewpoint, the inter-module connections are crucial since they affect the overall stability and resilience of the system [12, 13, 15, 16, 25]. The modules are fabricated in a controlled environment in a factory with high precision whereas the modules are connected on-site, which makes the inter-module connections highly susceptible to variables such as skilled labour, weather, availability of suitable equipment, etc. [11]. Various inter-module connection techniques have been proposed in the available literature that aims for easy and fast installations using bolts, shear key, plates, grouts, etc. [10, 11, 26]. The two forms of inter-module connections are horizontal connections and vertical connections. The floor beams of the upper modules and the ceiling beams of the lower modules are connected horizontally. For corner supported modules, the vertical connections involve joining the upper module to the

lower modules at corner columns. The most common methods for connecting the top and lower modules are shear keys with gusset plates or fastened gusset plates [27].

Based on the practical design for global analysis, several unique inter-module connections have been suggested, and simpler models have been used [4, 15, 27]. According to certain studies, there should be a frame element for horizontal connection at the floor beam level of the upper module and another frame element between the columns of the upper and lower modules [4]. Several studies have employed a spring element to simulate the stiffness characteristics of the connections [18, 27]. Fathieh and Mercan [28] suggested that the horizontal connection should be designed as a frame element with 30% stronger bending and shear strengths than the adjacent beam section. The vertical connection may be modelled by extending the centerlines of the columns beyond where they touch the beams and then joining them vertically to the lower columns. A popular approach to represent the response of the structure is to model the vertical connection as a rigid joint, as is suggested in certain literature [4]. However, this may not be a conservative approach as it may lead to extremities in the building response for development of plastic hinges in the columns. On the other hand, presuming the inter-module connections as pinned may result in severe sway behavior of the structure in comparison to a rigid-joint [18]. Assuming either a pin or a rigid connection can also lead to overestimating or underestimating the conventional K-factor based on the effective length [29]. As a result, it is considered that using the assumption of a pin joined inter-module connection is a safer method for a non-sway frame [30-32].

To overcome the drawbacks of conventional steel structures with rigid or pinned connections, comprehensive research on the progressive collapse and structural robustness of steel-concrete composite modular buildings was conducted in this work. Since experimental results for structural elements are cost effective and easily available than for modular buildings, a FE model for composite modular buildings was created by individually verifying the FE modelling

of structural elements. Nonlinear static and nonlinear time-history analysis were conducted for a typical 10-story modular structure under a sudden module removal scenario in ABAQUS software using alternate load path (ALP) method. CFST columns were used to replace conventional steel columns to provide resistance against progressive collapse by buckling of columns. A semi-rigid inter-module connection modelling approach was proposed with force-displacement and moment-rotation relationships to accurately model and predict the response of connections. The model was then used as the foundation for a comprehensive parametric analysis to evaluate the progressive collapse and structural robustness of modular structures using a variety of parameters, such as the impact of the floor slab, connections between modules, building height, and the location of removed modules.

2. Modelling methods

2.1. Semi-rigid connection modelling

Inter-module and intra-module connections are critical because they maintain structural robustness, and general stability of the modular building [10, 33]. In numerical modelling, fully rigid connections or pin connections are usually considered. However, these can either overestimate or underestimate the rotational stiffness of joints. A traditional spring connector model that illustrates the load transfer mechanism of a standard module connection is proposed here. As shown in Fig. 2, the connection involves zero-length connector elements for modelling the vertical connectivity of modules and a horizontal connector element joining the columns of the lower modules. The proposed connection approach is designed in accordance with a bolted gusset plate between the modules. The length of the horizontal connector is selected as the center to center spacing of columns including the gap between modules. The connectors are modelled as elements with 12 available degrees of freedom (DoF) (6 translations and 6 rotations) which can be specified based on the available connection type and design. Several techniques, including the Kishi-Chen three-parameter model [34], can be employed for

predicting the semi-rigid behavior of joints. The Kishi-Chen model shown in Fig. 3 contains three parameters: (a) initial connection stiffness (R_{ki}), (b) ultimate connection moment capacity (M_u) and (c) shape parameter (n). The moment-rotation relation of the Kishi–Chen model is defined as

$$M = \frac{R_{ki}\theta}{[1 + (|\theta|/\theta_0)^n]^{1/n}} \quad \text{where } \theta_0 = \frac{M_u}{R_{ki}} \tag{1}$$

2.2. Modelling of CFST columns

To investigate the accuracy of the CFST column numerically, a FE model using beam elements (B31) was developed in ABAQUS based on the approach presented by Wang et al. [22] and Tao et al. [35]. The beam element type B31 is a two-node, 3D Timoshenko element. The keyword *REBAR was used to assign the steel section as a material integration point. The geometric properties of the rebar were defined as the area and the coordinates of rebar with respect to the cross-section. The beam element was modelled as the concrete material and the steel box section was specified as rebar layer on the edges of the beam element as shown in Fig. 4 [22, 36]. The longitudinal strain at the material integration locations in the section was assumed to follow the linear strain assumption over the section depth. Since, the interaction between concrete infill and steel rebar cannot be defined for B31 elements, it is important to include the interaction effects while defining the uni-axial behavior of concrete and steel.

Steel models of many types can be used to demonstrate the elastic-plastic behavior of box steel section with infill. The conventional linear or bilinear stress-strain equation underestimates tension strength and overestimates compressive strength. The steel model proposed by Tao et al. [35] was used here to define the stress-strain curve which is highly influenced by the confinement factor (ξ_c). The confinement factor is defined as $\xi_c = A_s f_y / A_c f_c$, where A_s and A_c are the area of steel section and concrete infill, respectively. Due to the initial weak steel-concrete interaction, the effective curve of steel in rectangular CFST columns exhibit a linear

response in the elastic stage [37]. When the stress reaches its peak value, a significant interaction begins to develop, and the effective curves enter the post peak stage. The decreasing slopes of the curves vary based on the ξ_c value. The steel model takes into account the reduction of strength in axial direction due to development of hoop stress because of the lateral expansion of concrete. It also accounts for the steel yielding and the influence of local buckling. The stress-strain curve adopted here is a shown in Eq. (2).

$$\sigma = \begin{cases} E_s\varepsilon & for\ 0 < \varepsilon \le \varepsilon'_y \\ f'_{cr} - \left(f'_{cr} - f'_y\right)\left(\dfrac{\varepsilon'_{cr} - \varepsilon}{\varepsilon'_{cr} - \varepsilon'_y}\right)^{\psi} & for\ \varepsilon'_y < \varepsilon \le \varepsilon'_{cr} \\ f'_u - (f'_u - f'_{cr})\left(\dfrac{\varepsilon_u - \varepsilon}{\varepsilon_u - \varepsilon'_{cr}}\right)^{p} & for\ \varepsilon'_{cr} < \varepsilon \le \varepsilon_u \\ f'_u & for\ \varepsilon \ge \varepsilon_u \end{cases} \quad (2)$$

where E_s is the modulus of elasticity of steel, ε'_y is the strain corresponding to f'_y, taken as f'_y/E_s; and ε_u is the ultimate strain of steel corresponding to the ultimate strength (f_u).

Similarly, equations for the parameters, ultimate strain of steel corresponding to the ultimate strength (ε_u), initial peak stress (f'_y), strain corresponding to the peak stress of unconfined concrete (ε_{c0}), critical stress (f'_{cr}), critical strain (ε'_{cr}), stress corresponding to the ultimate steel strain (f'_u) and the exponents ψ and p are defined as follows.

$$\varepsilon_u = \begin{cases} 100\varepsilon_y & for\ f_y < 300\ \text{MPa} \\ \left[100 - 0.15\left(f_y - 300\right)\right]\varepsilon_y & for\ 300 < f_y \le 800\ \text{MPa} \\ \left[100 - 0.15\left(f_y - 300\right)\right]\varepsilon_y & for\ 800 < f_y \le 960\ \text{MPa} \end{cases} \quad (3)$$

$$\varepsilon_{c0} = 0.00076 + \sqrt{(0.626f'_c - 4.33) \times 10^{-7}} \quad (4)$$

$$\frac{f'_y}{f_y} = \left(1.6 + 42.5\left(\frac{D'}{10000t}f_y^{0.7}\right)^{7}\right)^{-0.1} + 0.02\left(\frac{\varepsilon_{c0}}{\varepsilon_y}\right)^{1.1} \quad (5)$$

$$\frac{f'_{cr}}{f_y} = 0.2 + 0.04\frac{B}{H} + \frac{0.56}{1 + \left(\left(\frac{D'}{t}(f'_c)^{0.1} - 22\right)\right)/120\Big)^{2}}\left(\frac{f_y}{f'_c}\right)^{0.06} \quad (6)$$

$$\varepsilon'_{cr} = \varepsilon_y \left[1 + 12.8 \left(\frac{D'}{t} (f'_c)^{0.7} \right)^{1.5} \xi_c^{1.8} \sqrt{f'_c} \frac{1}{(f_y)^{2.25}} \left(\frac{B}{H} \right)^{0.2} \right] \tag{7}$$

$$f'_u = f_y \left[\frac{6 + 4\xi_c + 0.015\, D'/t}{6 + 3.6\xi_c + 0.18\, D'/t} \right] \left(\frac{B}{H} \right)^{0.08} \left(\frac{f_y}{f'_c} \right)^{0.0025} \tag{8}$$

$$p = \begin{cases} 0.004E_s \left(\dfrac{\varepsilon_u - \varepsilon'_{cr}}{f'_u - f'_{cr}} \right) & for\ f'_u > f'_{cr} \\ -0.02E_s \left(\dfrac{\varepsilon_u - \varepsilon'_{cr}}{f'_u - f'_{cr}} \right) & for\ f'_u \le f'_{cr} \end{cases} \tag{9}$$

where ε_y is the yield strain of steel corresponding to the yield stress, taken as f_y/E_s. f'_c and f_y corresponds to the compressive strength of concrete and yield strength of steel, respectively. The ratio f'_y/f_y represents the initial intensity of the interaction between the steel tube and concrete in CFST columns. D' is defined as the diagonal distance between the outer corners of the cross section of rectangular CFST column, taken as $\sqrt{B^2 + H^2}$. The value of strain softening exponent (ψ) was suggested to be 1.5. The critical stress (f'_{cr}) accounts for the dilation effect of the infill concrete and the localized buckling of the steel tube. For rectangular steel section with $\xi_c < 2$, continuous strain softening is observed after the peak stress as shown in Fig. 5(a). Therefore, although the steel tube is modelled as a rebar, it acts as a box section because of the consideration of local buckling and hoop stress in the material definition.

The uniaxial stress-strain relationship of confined concrete was defined using the proposed equations by Tao et al. [35], which considers 5 parameters including the confined concrete strength (f'_{cc}) and corresponding ultimate strain (ε'_{cc}), residual stress (f_r), and coefficients *a* and *b*. It takes into account the enhancement of ductility and strength due to the passive confinement from the steel box section as shown in Fig. 5(b).

$$\sigma = \begin{cases} \dfrac{aX + bX^2}{1 + (a-2)X + (b+1)X^2} f'_{cc} & for\ X \le 1\ or\ (X > 1\ and\ \sigma > f_r) \\ f_r & for\ X > 1\ and\ \sigma \le f_r \end{cases} \tag{10}$$

where $X = \varepsilon/\varepsilon'_{cc}$. The size effect is prominent for rectangular CFST columns. Therefore, a strength correction factor γ_c is introduced to account for the size effect as a function of $D_c \left(= \sqrt{(B-2t)^2 + (H-2t)^2}\right)$.

$$\frac{f'_{cc}}{f'_c} = \gamma_c \left[0.845 + \frac{{f_y}^{0.08}}{2(f'_c)^{0.4}} + \frac{0.35(\xi_c)^{1.06}}{(D'/t)^{0.3}} \left(\frac{B}{H}\right)^{0.6}\right] \tag{11}$$

$$\gamma_c = \left(\frac{D_c}{212}\right)^{-0.14} \leq 1.05 \tag{12}$$

$$\varepsilon'_{cc} = 2500 + \left(283\xi_c^{1.4} - \frac{1.7 \times 10^7}{(D'/t)^{3.75}}\right)\left(\frac{B}{H} f'_c\right)^{0.3} + \frac{2.25 \times 10^8}{(D'/t)^4} \ (\mu\varepsilon) \tag{13}$$

$$\frac{f_r}{f'_{cc}} = 0.96\xi_c^{0.1} + \frac{9.7}{(D'/t)^{1.5}} + 0.09\sqrt{\frac{f_y}{f'_c}\frac{B}{H}} - 0.7 \qquad \leq 1 \ and \geq 0.15 \tag{14}$$

$$a = \alpha_1 \frac{E_c \varepsilon'_{cc}}{f'_{cc}} \tag{15}$$

$$\alpha_1 = 1 + 0.2\xi_c^{\left(0.05 + {}^{0.2}/_{\xi_c}\right)} \tag{16}$$

$$b = 0.15 - e^{(-1.4\xi_c^{0.8})} - 0.012\left(\frac{f'_c D'}{t}\right)^{0.3}\left(\frac{H}{B}\right)^2 \tag{17}$$

The tensile strength of infill concrete was not considered in the model as the tensile forces are resisted primarily by the steel section. The proposed stress-strain relationship has been extensively used to predict the uni-axial behavior of CFST columns along with the interaction between steel section and concrete infill. This approach to design of CFST columns improves the efficiency of the numerical simulation without compromising the accuracy.

2.3. Progressive collapse modelling

To study the gravity induced progressive collapse behavior of structures, the beam-shell modelling approach was adopted. The beams and columns were modelled as two-node beam elements (B31) [38], whilst the slab was modelled by a four-node shell element (S4R) [38]. Reinforcement in the shell element was provided using the rebar option by specifying the area

of steel and the distance from the mid-surface of slab [38]. The beam-to-column connection is modelled using a connector element. The floor slab was modelled to rest on top of the beams using rigid beam constraint equations. Previous research has found that the ceiling slab lacks sufficient in-plane stiffness to operate as a floor diaphragm for lateral load transmission [18]. As a result, its contribution was not accounted for in the frame modelling. The slab's concrete material was modelled as un-confined concrete using the concrete damaged plasticity model [38]. The stress strain curve was considered linear till $0.5f_{ck}$ and a parabolic curve was adopted as specified in EC2 [39].

$$\sigma = f_c \frac{kn - n^2}{1 + (k-2)n} \tag{18}$$

where $n = \varepsilon/\varepsilon_0$ and $k = 1.05E_c\varepsilon_0/f_c$. ε_o is the strain corresponding to peak stress f_c.

The progressive collapse analysis was conducted in 3 steps: (1) static load application, (2) dynamic removal of column, and (3) dynamic step for response stabilization. The structure was subjected to a load combinations as per the GSA [40]. To simulate the removed module, *MODEL CHANGE command was selected from ABAQUS library [38]. The module removal was conducted in a short duration of 0.02 sec to meet the requirement from GSA [40] which specifies the duration should be less than 10% of the fundamental period of the remaining structure.

3. Verification study

3.1. Semi-rigid connection

A steel frame with semi-rigid joints investigated by Stelmack [41] was selected to verify the ability of the connector element in predicting the semi-rigid behavior of the beam-column connection in frames. Stelmack [41] studied the behavior of a two-storey frame with bolted top and seat angles connections of L 4 x 4 x 1/2. The frame comprised of A36 W516 sections, and all columns were pinned supports at the bottom as shown in Fig. 6. The three parameters of the Kishi–Chen power model were calculated by curve fitting analysis for the experimental

moment-rotation curve as: R_{ki} = 4520 kNm/rad, M_u = 24.9 kNm and n = 0.91 [42]. Initially, a gravitational force of 10.68 kN was applied at one third points of the beam on the first floor. Lateral load was applied in the next step and the lateral load deflection curves were recorded. A similar model was replicated for the present study with similar components and loading scenarios. To simulate the semi-rigid behavior of beam column joint, the proposed zero-length semi-rigid connection modelling approach was adopted. The translational DoF and torsional rotation were modelled as rigid elements and the bending rotational DoFs were modelled using the Kishi-Chen model. Fig. 7 shows the comparison of lateral load deflection curves for the steel frame with semi-rigid joints. A good agreement between the experimental and simulation results was obtained which validates the accuracy of the connector element for predicting the behavior of semi-rigid joints in frames. Therefore, the similar connection approach was adopted for further investigations.

3.2. CFST column

To validate the modelling technique for CFST columns, typical experimentally tested CFST column specimens available in the literature were used. Table 1 shows the properties of the CFST columns used in the study, where B, H and t represents the width, depth, and thickness of the steel tube, respectively. The specimens under consideration comprised of members with varying ductility, slenderness ratios and strength of steel and infill concrete. It was observed from Table 1 that the FE beam model successfully predicted the behavior of CFST column subjected to axial loading with a mean value of 0.99 and coefficient of variation (CoV) of 0.038. The slight discrepancy in the result is obtained due to the material modelling of confined concrete as compared to the experimental values. Fig. 8 shows the load deflection curves for typical box section CFST columns. It was concluded that the model successfully predicted the precise behavior of peak load, and the behavior of column post concrete cracking. Therefore, the same material model was used for further modelling and investigation of modular buildings.

3.3. Progressive failure analysis for conventional steel building

A 20-storey steel building investigated by [5] was selected to verify the numerical model predicting the progressive collapse behavior of multi-storey building subjected to column removal scenarios using ALP method. Fu [5, 23] studied the behavior of a conventional tall building subjected to column loss scenarios using the software ABAQUS and ETABS as shown in Fig. 9. The frame construction consisted of a 20-storey structure with 7.5 m grid spacing in both directions. The floor height was 3 m, and cross bracings were used to enhance lateral stability. The beam, column, bracing and slab sections were modelled similar to the cross-sections used by Fu [5, 23]. The concrete slab was modelled as a shell element with A252 mesh reinforcement as a smeared layer. Rigid beam constraints were used to connect the slab to the beams. Beam-to-column joints were designed as completely pin connections. The composite slab across the top of the connection offered continuity throughout the connection, and the connection acted as a semi-rigid connection. According to the earlier version of GSA rules, the structure was subjected to dead load of the slab and 25% of the live load [43]. The structure was assumed to be fixed at the bottom.

Fig. 10(a) and Fig. 10(b) show the comparison between the displacement-time history of the node above the removed column and the axial force in the column next to the removed column, respectively. Oscillating responses were recorded due to the removal of column in a duration less than the natural time period (almost 10% of the natural time period) of the structure which in turns produces dynamic response of the structure. The instantaneous column removal can occur due to explosions which can be similar to application of an instantaneous vertical downward force at the location. A good agreement between results was obtained. The present modelling approach was able to predict the structural response of the building in scenarios of column removal, and therefore, this approach was later employed to examine the progressive collapse behaviour of composite modular buildings.

4. Case study of a composite modular building

4.1 Modelling of composite modular building

A 10-story office steel-concrete composite modular building with CFST columns was modelled in the FE software ABAQUS, as shown in Fig. 11(a). The dimensions of the modular unit were chosen as 6 x 3 x 3.3 m based on the commercially available module sizes as shown in Fig. 11(b) [11]. Corner supported modules were used to design the modular building that are connected at the corner joints. The structure was designed as per the Australian design standard AS/NZS 2327[44]. The size of structural elements was determined for the load case of 1.5 (D.L + L.L) and are shown in Table 2 [40, 45]. The dead loads and live loads were taken as per the ASCE-7:2002 [45] guidelines for office buildings as shown in Table 3.

FE modelling of the structure was conducted based on the proposed modelling methods. The main reinforcement provided in the slab is the A252 mesh acting at 30 mm from the top of the slab and a 0.9 mm thick metal deck at the bottom of the slab. This reinforcement is specified in both slab directions and acts as a smeared layer. The rebar mesh and sheeting for the slab were modelled as steel sections. The concrete material and steel box section for CFST column were modelled using the equations proposed by Tao et al. [35].

The proposed inter-module connection was used in this study. The rotational DoFs were defined using the moment-rotation relationships depending upon the connection type. The translational DoFs for the vertical connections were considered as rigid. The axial and shear stiffness of the gusset plate were calculated mathematically using the Eqs. (7) and (8), where A is the cross-section area, E is the elastic modulus, G is the shear modulus and L is the length of the gusset plate between the centreline of column. To simulate the rigid behaviour of the horizontal and vertical connections, the rotational DoFs were defined as rigid connectors. For pined connections, the axial and torsional rotational stiffness was considered as infinite, whereas the rotational stiffness was considered as zero. To simulate the progressive collapse,

different module loss scenarios were considered. The module was removed in a dynamic step of 0.02 sec. The structure was then observed for 5 sec after the module removal to plot the dynamic vibrations or report any failures in the structure.

$$k_{axial} = \frac{AE}{L} \tag{19}$$

$$k_{shear} = \frac{AG}{L} \tag{20}$$

4.2 Assessment methodology

Nonlinear static pushover and dynamic analyses were conducted using the ALP method to explore the progressive collapse response of the composite modular building in module removal scenarios subjected to gravity loads [40]. Nonlinear static pushover analysis provides valuable knowledge on the capacity curve of the building as well as examine failure scenarios. The initially damaged building is subjected to an increasing gravity load in the pushover analysis until the building collapses. The module under consideration is removed statically, as indicated in Fig. 12(b), and then an increased design gravity load, DAF(1.2DL+0.5LL), is applied to the floors above the damaged module. The GSA guidelines suggests maximum value of DAF = 2 for column removal scenarios which is used in the study for module removal scenarios as well [40]. The nonlinear dynamic analysis considers the effects of both nonlinear material and geometrical nonlinearity along with the effect of dynamic actions, inertia, and structural damping. As a result, this analysis produces the most reliable results, but at a significant computing expense. GSA guidelines employs the nonlinear dynamic analysis to confirm that a building has sufficient resistance against progressive collapse due to gravity load combination of (1.2 DL + 0.5 LL) as shown in Fig. 12(a) [40]. The failure criteria adopted herewith is the ultimate failure of the modular building which is initiated by the shear failure of the gusset plate or the buckling of adjacent column.

4.3 Rigid versus pinned inter-module connections

Progressive collapse of the modular building was simulated using the nonlinear dynamic analysis procedure recommended in GSA [40]. Lateral load was not considered in this study. Fig. 13 shows the results for the maximum vertical displacement observed for modular building with rigid and pinned inter-module connections. The displacement values are observed at the node above the removed module with maximum displacement in the structure. The maximum displacement for the rigid connection is 20.7 mm, whereas for the pinned connection is 31.34 mm just after removal of the module. The displacement amplitude reduces with time in the next 5 seconds. The amplitude of the pinned connection, however, shows lower amplitude reduction with time. This can be attributed to the available rotational DoF at the inter-module connection compared to constrained DoF in a rigid connection.

The locations of plastic hinge formation were also evaluated for the dynamic analysis of the building as shown in Fig. 14(a) and Fig. 14(b). The primary load transfer element after a module removal is the gusset plate/horizontal inter-module connection in the horizontal direction provided between adjacent columns. As a result, the plastic hinges in a rigid connection are primary developed in the columns that are a part of the vertical inter-module connection. The plastic hinges shown in Fig. 14 are primarily caused due to cracking of concrete in compression. However, the overall CFST column has not reached the failure state, instead, local buckling was observed near the joint itself. It was noted that a more plastic hinges were developed in adjacent columns along the shorter span of the modular building. This can be attributed to the floor slab aspect ratio of the upper module and the transfer of moments to the nearest column, in the vicinity of the thus formed cantilever structure.

5. Parametric study

5.1 Module versus column removal

Existing research in the field of progressive collapse analysis has been based on the column removal scenarios for conventional buildings as dictated by the GSA design guidelines. Therefore, to establish the critical scenario for a modular building, a corner module and a corner column removal scenario were compared. The proposed inter-module connection was considered as a pin jointed connection. It was observed from Fig. 15 that the module removal scenario resulted in higher displacement values for the structure. Plastic hinge formation was also observed in the corner module removal scenario whereas no plastic hinge was developed in case of corner column removal. Therefore, it was concluded that the module removal scenario is more critical and lead to a more catastrophic damage compared to a column removal scenario.

5.2 Location of removed module

The structural response of the 10-storey composite modular structure was investigated subjected to module loss scenarios at several positions: (a) corner, (b) middle of the shorter span, and (c) internal as illustrated in Fig. 16. The following locations are selected based on the suggestions provided in GSA for column loss scenarios. The proposed inter-module connection was considered as a pin jointed connection. The structural response was evaluated based on both nonlinear dynamic and static pushover analysis.

The time-displacement curve for nonlinear dynamic analysis under various module removal cases is shown in Fig. 17. Following the sudden removal of module at 1.02 seconds, the vertical displacement increases considerably to its maximum value, followed by a reduction in amplitude due to damping, till the structure reaches a new state of equilibrium. It was observed from the results that the corner module removal shows the highest vertical deflection of

31.34 mm, whereas the maximum vertical displacement is quite similar for mid span and internal module removal. The maximum displacement for mid span module removal is 8.39 mm and for internal module is 8.35 mm. The overall deformation of the structure is observed primarily in the storeys above the removed module. It was observed that only one plastic hinge is formed in the corner module removal case because of cracking of concrete in compression near the vertical connection. Whereas no plastic hinge formation was observed in the case for mid span and internal module removal. Thus, the structure is considered not susceptible to progressive collapse according to GSA criteria.

Nonlinear static analysis shows that neither progressive failure nor member failure is observed for DAF value of 2 as suggested by the GSA. Therefore, the inclusion of CFST columns significantly improves the strength and in general, the buckling strength of adjacent columns. However, it was observed that the DAF value of 2 significantly overestimates the response of building compared to nonlinear dynamic analysis as shown in Fig. 17. Based on the location of module removal scenarios, DAF values of 1.65 for corner module and 1.2 for internal as well as the edge module has been suggested.

5.3 Effect of floor slab

The primary horizontal load path for a conventional building consists of force transfer between beams where the continuous slab act as a rigid diaphragm. Whereas for a modular building, the force transfer between the columns and horizontal inter-module connection/gusset plate makes up the primary horizontal load path. To study the effect of discrete floor slabs available in a modular building, two cases of with and without the floor slabs were analysed. The equivalent weight of the slab and the loads were applied as line loads on the floor beams. Fig. 18 shows the displacement time-history of modular building with and without the inclusion of the floor slab. As observed from the figure, the maximum displacement for no slab case is 68.5 mm, which is significantly higher than that of the modular building with floor slab. In comparison

to a traditional rigid frame where the continuity across a floor allows the slab to act as a rigid diaphragm, modular buildings show different behaviour due to the structural discontinuity between modules. It is observed that the floor slabs work as multiple diaphragms for modular building if the inter-module connections are accurately constructed. Therefore, it was concluded that the rigid diaphragm effect of the slab contributes highly to the response of modular buildings and should be considered while evaluating the response of modular structures.

5.4 Effect of semi-rigid behaviour of inter-module connections

The effect of moment-rotation relationship for horizontal inter-module connection was investigated using the fixity factor (*f*) variation [46]. Fixity factor can be expressed in terms of initial stiffness of the connection (R_{ki}) and the element stiffness (EI/L) as shown in Eq. (9). The value of fixity factor varies from 0 for a pin connection to 1 for a rigid connection. Therefore, to investigate the effect of the stiffness of semi-rigid connections, the fixity factor *f* is varied from 0 to 1, whilst the ultimate moment capacity (M_u) and the shape parameter (n) are kept constant as shown in Fig. 19.

$$f = \frac{1}{1 + \frac{3EI}{R_{ki}L}} \tag{21}$$

Fig. 20 shows variation of maximum displacement observed in nonlinear dynamic analysis for various fixity factor values. The maximum displacement observed for semi-rigid connections was 29 mm which is quite similar to the pinned inter-module connection for corner module removal. Fig. 21 shows the displacement time history response for modular building with a typical semi-rigid connection with f = 0.5 compared to rigid and pin connections. It was therefore concluded that the rotational DoFs have very little effect for non-sway frame frames under gravity induced progressive collapse. The steel gusset plate of 25 mm thickness has insufficient rotational stiffness compared to the translational stiffness in axial and shear

directions which was also observed from the small variation of displacement for various fixity factor values. The rigid connection approach is avoided here as it leads to overestimation of the number of plastic hinges developed within the structure.

5.5 Effect of gusset plates

The nonlinear dynamic analysis for the corner module removal scenario was used to study the forces generated in the horizontal inter-module connection. Fig. 22(a) and Fig. 22(b) provide the values of maximum shear forces and axial forces developed in the connection, respectively. Since the module is removed from the ground floor, the forces from the upper modules cannot be directly transferred to the foundation. Therefore, the forces are transferred via the gusset plates into the adjacent columns and thereafter the adjacent beams. This leads to deflection of the gusset plate with the development of axial and shear forces. It was observed that the horizontal shear forces were negligible and did not contribute enough to the connection capacity. As observed from Fig. 22, the magnitude of vertical shear forces is significantly higher than the axial forces. Steel gusset plate having lower value of shear strength, have a higher tendency to fail due to the shear forces developed after module removal. Therefore, a nonlinear static pushover analysis was conducted to evaluate the value of load factor for the modular building against progressive collapse due to failure of gusset plate in shear. The load factor has been defined similar to DAF wherein the load factor is the ratio of the applied load at failure to the dynamic load specified as per GSA guidelines.

A nonlinear static pushover analysis was conducted on the modular building with different gusset plate sizes to study the failure mechanism of the structure under corner module loss scenarios. The dimensions of the gusset plate under consideration were 5 mm, 10 mm, and 25 mm. The axial and shear stiffness properties for the horizontal inter-module connection corresponding to the plate dimensions were provided. Damage and failure criteria were provided from the ABAQUS connector library, and the plates were considered to fail

predominantly in vertical shear. Once the failure had occurred in the gusset plate/ horizontal connector, all other constrained DoFs were also released. The shear strength of the plate was evaluated according to the Von Mises criterion.

Fig. 23 shows the load factor vs vertical displacement curve for different sizes of gusset plate in a corner module removal scenario. The load factor, α has a value of 0.97 for 5 mm plate, 3.04 for a 10 mm plate and 4.05 for a 25 mm plate. All the curves have a similar slope for load factor vs displacement curve but show different failure mechanisms. The modular building with 5 mm and 10 mm plate showed progressive failure by the failure of gusset plate in shear at a maximum vertical displacement of 19 mm and 92 mm, respectively with local buckling of adjacent column along the shorter span near connection. For modular building with 25 mm plate, buckling of adjacent column was observed at a load factor of 3.51 and then failure of gusset plate was observed at a load factor of 4.05. Fig. 24 shows the initial failure mechanism for a 25 mm gusset plate showing the global buckling of adjacent column before the failure of gusset plate. Fig. 25 shows the axial load versus displacement curve for the adjacent column subjected to global buckling by crushing of concrete. The curve showed similar behaviour to the validation study for the CFST column. It was observed that the CFST columns provided higher buckling strength as compared to a steel or a reinforced concrete column. The buckling and the post buckling strength of CFST columns played a major role in preventing the progressive collapse of the modular structure whereas the conventional steel columns failed to arrest the failure as observed from similar studies [4, 9]. The CFST columns provides an advantage in designing smaller sized sections for modules which are limited in space due to the transportation constraint. Therefore, it was concluded that, with adequate capacity of horizontal gusset plate, sufficient resistance against progressive collapse of a modular building can be achieved. Hence, providing 5 mm gusset plate will not be sufficient to resist the collapse of structure. Whereas, providing a gusset plate of 10 mm or 25 mm thickness will provide

sufficient capacity against progressive collapse depending on the buckling capacity of the adjacent column.

5.6 Effect of building height

This study investigates the effect of modular building height ranging from 10 to 30 storeys. Nonlinear dynamic and static analysis were conducted for corner module removal to evaluate the value of DAF. Similar floor layout was used to develop FE models for 20 storey and 30 storey modular building for gravity loads. Fig. 26 shows the time displacement response for corner module removal scenario. The observed DAF values were 1.44 and 1.34 for 20 and 30 storey building, respectively. It was observed that the DAF value reduces with the increase in height of the structure due to increase of overall load on structure. Therefore, the DAF value of 1.65 for corner module removal from the 10-storey building has been suggested to estimate the maximum response of composite modular buildings from nonlinear static analysis.

6. Conclusions

This paper investigated the progressive collapse behaviour of a 10-storey composite modular buildings using the nonlinear dynamic and static pushover analyses. The bridging ability and structural resistance of the building due to module removal from the ground floor were investigated using the ALP approach. The effect of slab, semi-rigid inter-module connection, and connection failure scenarios were also investigated. The numerical model successfully predicted the response of 10-storey composite modular building to progressive failure. Based on the results and conclusions, the DAF values for composite modular buildings have been suggested to accurately obtain the capacity curves from non-linear static analysis. The major conclusions and recommendations of the investigations are presented here.

1. The 10-story composite modular building was determined to be adequately resistant against progressive collapse caused by various module removal scenarios. It has been observed that a DAF value of 2.0 according to the GSA guidelines for nonlinear static

pushover analysis is deemed too high and conservative in predicting the progressive failure resistance of a modular building. Based on the location of module removal scenarios, DAF values of 1.65 for corner module and 1.2 for internal as well as the edge module has been suggested. The DAF value reduces with increase of building height.

2. The outcomes demonstrated the excellent capability of the suggested composite modular system with CFST columns to avoid gravity-induced progressive collapse following the sudden module removal. Even though plastic hinge formation is observed due to cracking of concrete in CFST column, the structure has sufficient strength and available alternate load paths to prevent extreme collapse.
3. The plastic hinges were formed in the adjacent columns in the direction of shorter span of the modules in the nonlinear dynamic analysis. It can be concluded that the gusset plates along the shorter span have higher role in redistributing the load to adjacent columns due to module removal.
4. It was observed that the corner module removal case is the most severe case compared to other locations as higher displacement values and a higher number of plastic hinges were observed for this scenario. The module removal scenarios were observed to be more critical compared to column removal even though the probability of occurrence of column removal is higher than module removal.
5. The floor slabs work as multiple diaphragms for modular building and provide rigidity and better load distribution even though it provides structural discontinuity in the structure.
6. The study of semi-rigid inter-module connection claimed that the rotational DoFs have very little effect for non-sway frames under gravity induced progressive collapse. Therefore, an assumption of a pin-jointed inter-module connection is a conservative approach to modelling of non-sway frames.

7. The horizontal inter-module connection/gusset plate resisted and transferred the loads primarily by vertical shear. Higher values of shear force were observed in the gusset plates as compared to axial force in the gusset plate attached to the removed module.
8. The failure mechanism for the modular building generally started with the shear failure of gusset plate if a 5 mm or 10 mm gusset plate is provided. For 25 mm gusset plate, global buckling of adjacent column was observed prior to the shear failure of gusset plates.

The current research is limited to a 10-storey composite modular building without the consideration of wind loads and subsequently, shear walls. The future research involves the investigation of tall composite modular buildings with shear walls and base structure.

Acknowledgements

This research was funded by the Australian Research Council (ARC) under its Future Fellowship Scheme (Project No: FT200100024). The financial assistance is gratefully acknowledged.

References

[1] Lawson M, Ogden R, Goodier C. Design in Modular Construction. Florida: CRC Press, Taylor & Francis Group; 2014.

[2] Adam JM, Parisi F, Sagaseta J, Lu X. Research and practice on progressive collapse and robustness of building structures in the 21st century. Engineering Structures 2018;173:122-149.

[3] Fu F. Structural Analysis and Design to Prevent Disproportionate Collapse. Boca Raton: CRC Press Taylor & Francis Group; 2016.

[4] Luo FJ, Bai Y, Hou J, Huang Y. Progressive collapse analysis and structural robustness of steel-framed modular buildings. Engineering Failure Analysis 2019;104:643-656.

[5] Fu F. Progressive collapse analysis of high-rise building with 3-D finite element modeling method. Journal of Constructional Steel Research 2009;65:1269-1278.

[6] Tran H, Thai H-T, Ngo T, Uy B, Li D, Mo J. Nonlinear inelastic simulation of high-rise buildings with innovative composite coupling shear walls and CFST columns. The Structural Design of Tall and Special Buildings 2021;30:e1883.

[7] Gao S, Guo L. Progressive collapse analysis of 20-storey building considering composite action of floor slab. International Journal of Steel Structures 2015;15:447-458.

[8] Kim J, Jung M. Progressive collapse-resisting capacity of modular mega-frame buildings. The Structural Design of Tall and Special Buildings 2013;22:471-484.

[9] Thai H-T, Ho QV, Li W, Ngo T. Progressive collapse and robustness of modular high-rise buildings. Structure and Infrastructure Engineering 2021:1-13.

[10] Lacey AW, Chen W, Hao H, Bi K. Structural response of modular buildings – An overview. Journal of Building Engineering 2018;16:45-56.

[11] Thai H-T, Ngo T, Uy B. A review on modular construction for high-rise buildings. Structures 2020;28:1265-1290.

[12] Chen Z, Khan K, Khan A, Javed K, Liu J. Exploration of the multidirectional stability and response of prefabricated volumetric modular steel structures. Journal of Constructional Steel Research 2021;184:106826.

[13] Chen Z, Wang J, Liu J, Khan K. Seismic behavior and moment transfer capacity of an innovative self-locking inter-module connection for modular steel building. Engineering Structures 2021;245:112978.

[14] Srisangeerthanan S, Hashemi MJ, Rajeev P, Gad E, Fernando S. Review of performance requirements for inter-module connections in multi-story modular buildings. Journal of Building Engineering 2020;28:101087.

[15] Alembagheri M, Sharafi P, Hajirezaei R, Samali B. Collapse capacity of modular steel buildings subject to module loss scenarios: The role of inter-module connections. Engineering Structures 2020;210:110373.

[16] Peng J, Hou C, Shen L. Lateral resistance of multi-story modular buildings using tenon-connected inter-module connections. Journal of Constructional Steel Research 2021;177:106453.

[17] Peng J, Hou C, Shen L. Progressive collapse analysis of corner-supported composite modular buildings. Journal of Building Engineering 2022;48:103977.

[18] Chua YS, Pang SD, Liew JYR, Dai Z. Robustness of inter-module connections and steel modular buildings under column loss scenarios. Journal of Building Engineering 2022;47:103888.

[19] Wegmuller AW, Amer HN. Nonlinear response of composite steel-concrete bridges. Computers & Structures 1977;7:161-169.

[20] Hirst MJS, Yeo MF. The analysis of composite beams using standard finite element programs. Computers & Structures 1980;11:233-237.

[21] Nie J, Tao M, Cai CS, Chen G. Modeling and investigation of elasto-plastic behavior of steel–concrete composite frame systems. Journal of Constructional Steel Research 2011;67:1973-1984.

[22] Wang Y-h, Nie J-g, Cai CS. Numerical modeling on concrete structures and steel–concrete composite frame structures. Composites Part B: Engineering 2013;51:58-67.

[23] Fu F. 3-D nonlinear dynamic progressive collapse analysis of multi-storey steel composite frame buildings — Parametric study. Engineering Structures 2010;32:3974-3980.

[24] Alembagheri M, Sharafi P, Hajirezaei R, Tao Z. Anti-collapse resistance mechanisms in corner-supported modular steel buildings. Journal of Constructional Steel Research 2020;170:106083.

[25] He X-H-C, Chan T-M, Chung K-F. Effect of inter-module connections on progressive collapse behaviour of MiC structures. Journal of Constructional Steel Research 2021;185:106823.

[26] Liew JYR, Chua YS, Dai Z. Steel concrete composite systems for modular construction of high-rise buildings. Structures 2019;21:135-149.

[27] Chua YS, Liew JYR, Pang SD. Modelling of connections and lateral behavior of high-rise modular steel buildings. Journal of Constructional Steel Research 2020;166:105901.

[28] Fathieh A, Mercan O. Seismic evaluation of modular steel buildings. Engineering Structures 2016;122:83-92.

[29] Singh ND, & Wahane, A. A Study on Buckling Analysis on CFST Columns with Different Slenderness Ratio & RCC Columns using ANSYS. International Journal for Research in Applied Science & Engineering Technology (IJRASET) 2020.

[30] Dai X-M, Zong L, Ding Y, Li Z-X. Experimental study on seismic behavior of a novel plug-in self-lock joint for modular steel construction. Engineering Structures 2019;181:143-164.

[31] Cao K, Li GQ, Lu Y. Stability analysis of non-sway modular frame with semi-rigid connection. J Archit Civ Eng 2016;33:83-89.

[32] Li G-Q, Cao K, Lu Y. Column effective lengths in sway-permitted modular steel-frame buildings. Proceedings of the Institution of Civil Engineers - Structures and Buildings 2019;172:30-41.

[33] Lacey AW, Chen W, Hao H, Bi K. Review of bolted inter-module connections in modular steel buildings. Journal of Building Engineering 2019;23:207-219.

[34] Kishi N, Chen WF. Moment Rotation Relations of Semirigid Connections with Angles. Journal of Structural Engineering 1990;116:1813-1834.

[35] Tao Z, Katwal U, Uy B, Wang W-D. Simplified Nonlinear Simulation of Rectangular Concrete-Filled Steel Tubular Columns. Journal of Structural Engineering 2021;147:04021061.

[36] Shi Y-L, Li H-W, Wang W-D, Hou C. A Fiber Model Based on Secondary Development of ABAQUS for Elastic–Plastic Analysis. International Journal of Steel Structures 2018;18:1560-1576.

[37] Han L-H, Li W, Bjorhovde R. Developments and advanced applications of concrete-filled steel tubular (CFST) structures: Members. Journal of Constructional Steel Research 2014;100:211-228.

[38] Smith M. ABAQUS/Standard User's Manual, Version 6.9. Providence, RI: Dassault Systèmes Simulia Corp.; 2009.

[39] C.E.N.-European Committee for Standardization. Eurocode 2: Design of concrete structures - Part 1-1: General rules and rules for buildings. Brussels; 2004.

[40] General Services Administration GSA. Alternate path analysis & design guidelines for progressive collapse resistance. Washington, DC; 2013.

[41] Stelmack TW, Marley MJ, Gerstle KH. Analysis and Tests of Flexibly Connected Steel Frames. Journal of Structural Engineering 1986;112:1573-1588.

[42] Kim S-E, Choi S-H. Practical advanced analysis for semi-rigid space frames. International Journal of Solids and Structures 2001;38:9111-9131.

[43] General Services Administration GSA. Progressive collapse analysis and design guidelines for new federal office buildings and major modernization projects. Washington, DC; 2003.

[44] Standards Australia. AS/NZS-2327 Composite structures. Composite steel-concrete construction in buildings. Australia; 2017.

[45] American Society of Civil Engineers ASCE. ASCE 7- Minimum design loads for buildings and other structures. Virginia: American Society of Civil Engineers; 2002.

[46] Thai H-T, Uy B, Kang W-H, Hicks S. System reliability evaluation of steel frames with semi-rigid connections. Journal of Constructional Steel Research 2016;121:29-39.

[47] Liu D, Gho W-M. Axial load behaviour of high-strength rectangular concrete-filled steel tubular stub columns. Thin-Walled Structures 2005;43:1131-1142.

[48] Tao Z, Uy B, Han L-H, Wang Z-B. Analysis and design of concrete-filled stiffened thin-walled steel tubular columns under axial compression. Thin-Walled Structures 2009;47:1544-1556.

[49] Tomii M. Experimental Studies on Concrete Filled Steel Tubular Stub Columns under Concentric Loading. Proceedings of International Colloquium on Stability of Structures Under Static and Dynamic Loads, SSRC/ASCE/Washington, D.C. 1977.

[50] Liew JYR, Xiong DX, Zhang MH. Experimental studies on concrete filled tubes with ultra-high strength materials. Paper presented at: 6th International Symposium on Steel Structures, 2011; Seoul, Korea.

[51] Schneider SP. Axially Loaded Concrete-Filled Steel Tubes. Journal of Structural Engineering 1998;124:1125-1138.

[52] Liu D, Gho W-M, Yuan J. Ultimate capacity of high-strength rectangular concrete-filled steel hollow section stub columns. Journal of Constructional Steel Research 2003;59:1499-1515.

[53] Yan Y, Xu L, Li B, Chi Y, Yu M, Zhou K, Song Y. Axial behavior of ultra-high performance concrete (UHPC) filled stocky steel tubes with square sections. Journal of Constructional Steel Research 2019;158:417-428.

[54] Xiong M-X, Xiong D-X, Liew JYR. Axial performance of short concrete filled steel tubes with high- and ultra-high- strength materials. Engineering Structures 2017;136:494-510.

Table 1. Properties of CFST column and the predicted ultimate axial capacity

Specimen	B (mm)	H (mm)	t (mm)	H/t	f_y (MPa)	f_c' (MPa)	$P_{u,exp}$ (kN)	$P_{u,sim}$ (kN)	$P_{u,sim}/P_{u,exp}$	Ref.
A5-1	100	130	5.8	22.4	300	106	1942.6	1947.12	1.01	[47]
UNC-H	250	250	2.5	100	338	40.9	3206.4	3314.74	1.03	[48]
3MN	150	150	3.2	46.8	300	27.8	1155.4	1115.74	0.97	[49]
SSH1-2	150	150	8	18.7	779	157	6830.5	6337.38	0.92	[50]
R4	102	152	4.57	33.3	365	23.8	1219.4	1161.44	0.95	[51]
sczs2-2-4	140	140	5.86	23.9	321	36.5	1762.4	1751.42	0.99	[37]
C3	181.2	182.8	4.18	43.7	550	60.8	3593.4	3592	0.99	[52]
S16-18-140	100	100	18.5	5.4	444.6	128.1	3749.1	3885.91	1.03	[53]
S14-14-120	100	100	14.2	7	468.6	111.3	3006.1	3062	1.02	[53]
S2	150	150	8	18.7	779	152.4	6773.9	6409.62	0.95	[54]
Mean									0.99	
CoV									0.038	

Table 2. Member sizes and material used in the model

Member	Material	Section size
Ceiling beam	S355	SHS 100x100x5 mm
Floor beam	S355	RHS 150x100x10 mm
Column	S355 (Steel box section) f_{ck} = 60 MPa (Unconfined concrete strength)	SHS 150x150x8 mm
Floor slab	S355 (Steel rebar and bottom plate) f_{ck} = 60 MPa (Concrete strength)	A252 rebar mesh 0.9 mm steel plate 130 mm concrete
Tie plate	S460	175 mmx25 mm

Table 3. Loading details for an office building as per ASCE-7:2002 [45]

Component	Load type	Load
Floor slab	Dead load Floor finish Live load	Gravity load 1 kN/m^2 2.5 kN/m^2
Floor beam	Dead load	Gravity load
Ceiling beam	Dead load	Gravity load

Column	Dead load	Gravity load

(a) Ronan Point building, 1968 (b) World Trade Centre, 2001

Fig. 1. Progressive collapse of structures

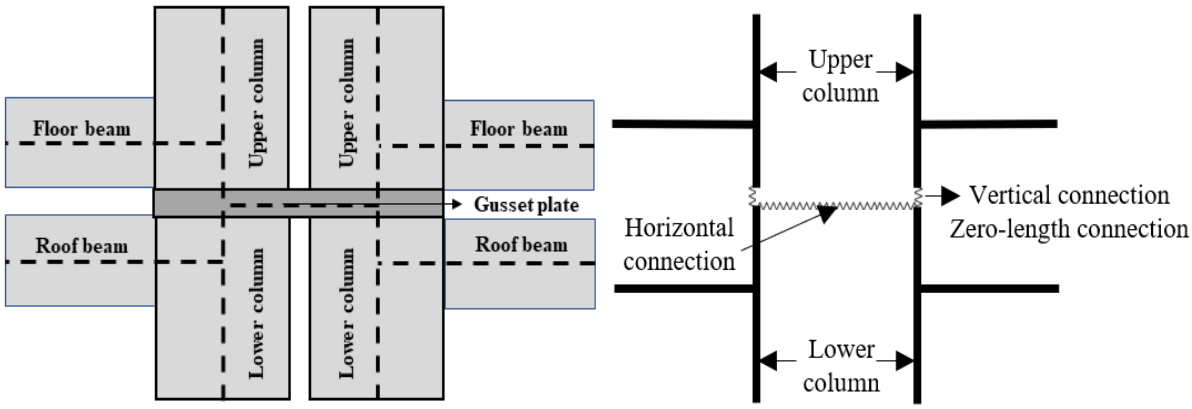

(a) Connection detail (b) Simplified connection model

Fig. 2. Schematic view of inter-module connection

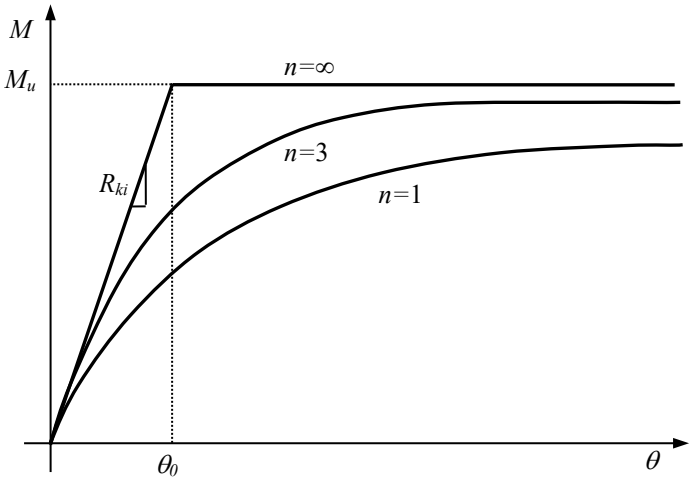

Fig. 3. Kishi-Chen model

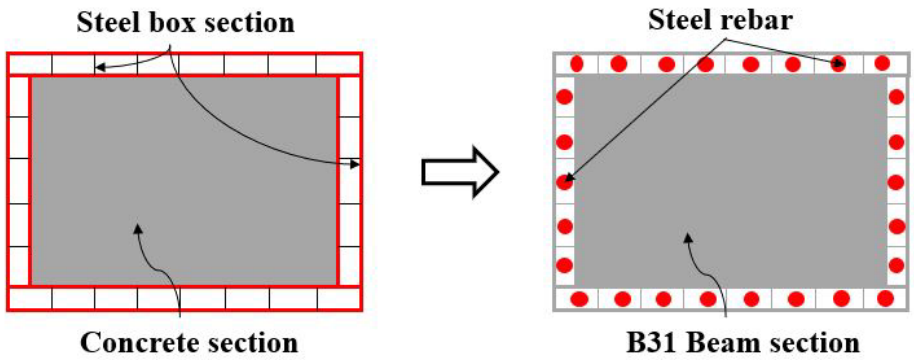

Fig. 4. Modelling approach for CFST column with B31 beam element in ABAQUS

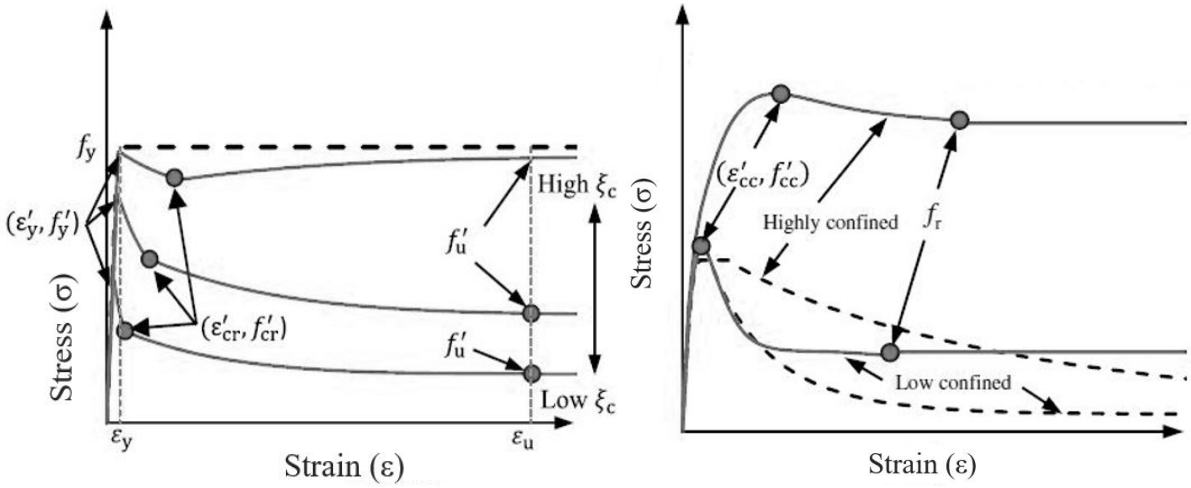

(a) Steel box section (b) Concrete infill

Fig. 5. Material models for CFST column [35]

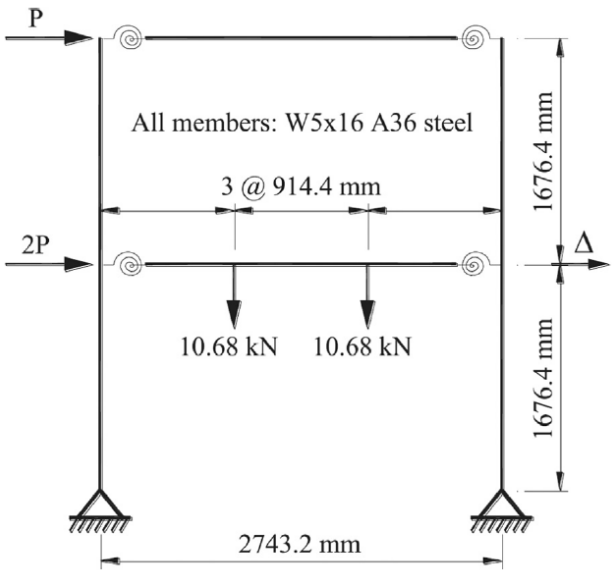

Fig. 6. Stelmack's two-storey planar frame with semi-rigid connections [41]

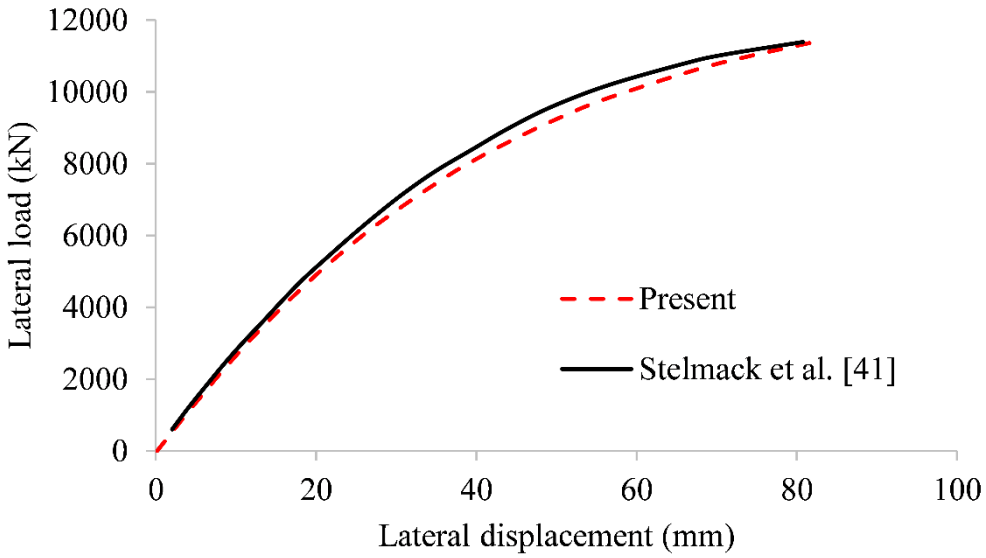

Fig. 7. Comparison of results of lateral load vs lateral displacement

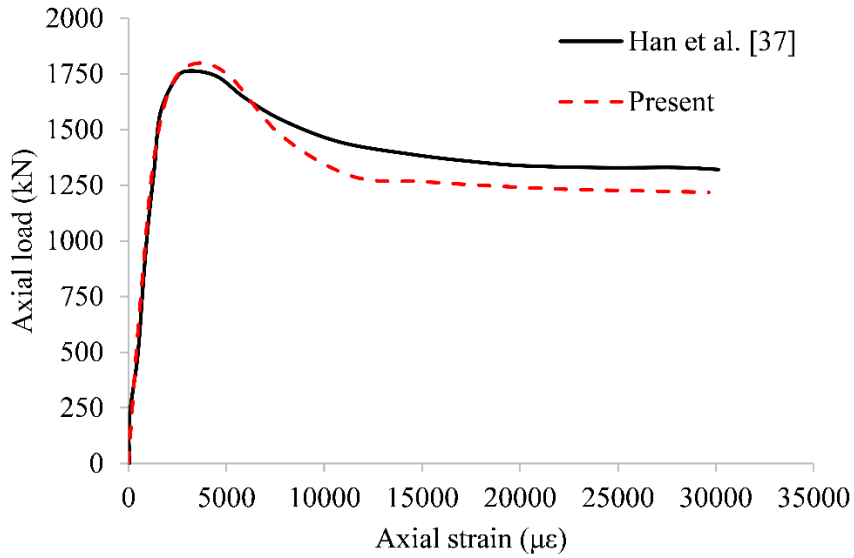

(a) sczs2-2-4

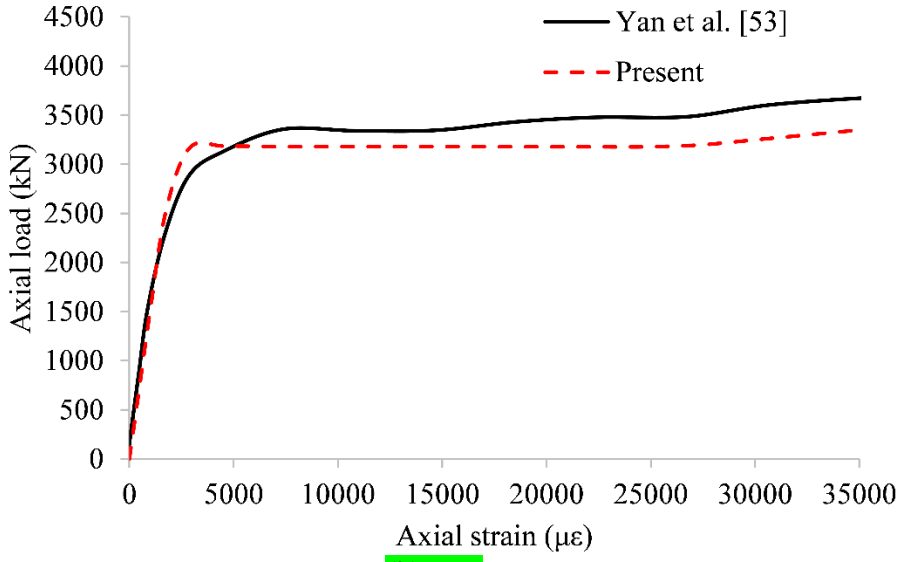

(b) S16

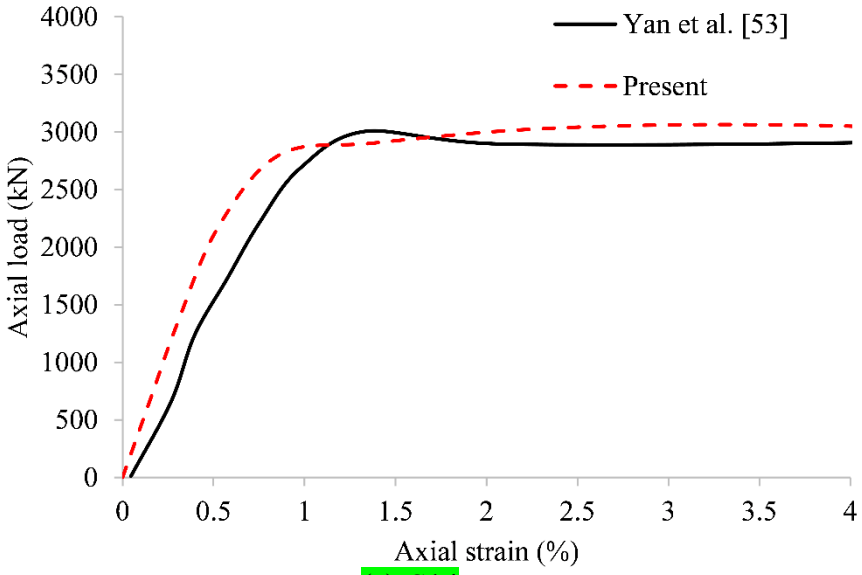

(c) S14

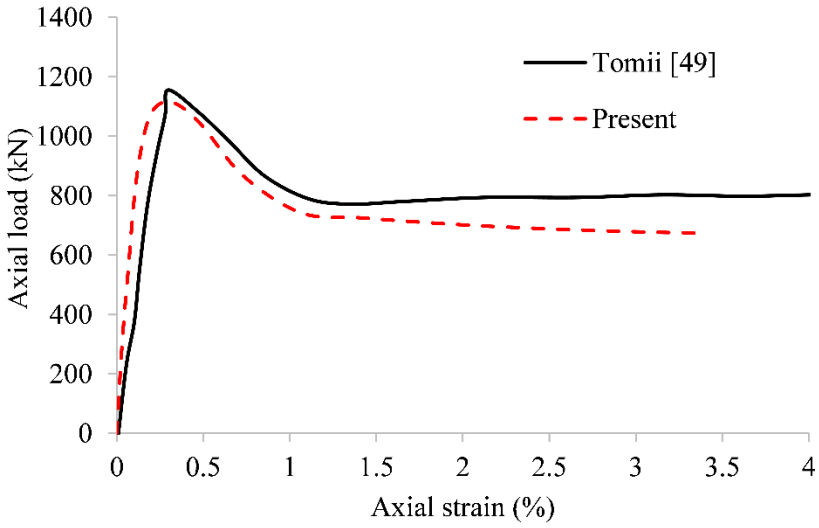

(d) 3MN

Fig. 8. Comparison of load deformation curves for CFST columns

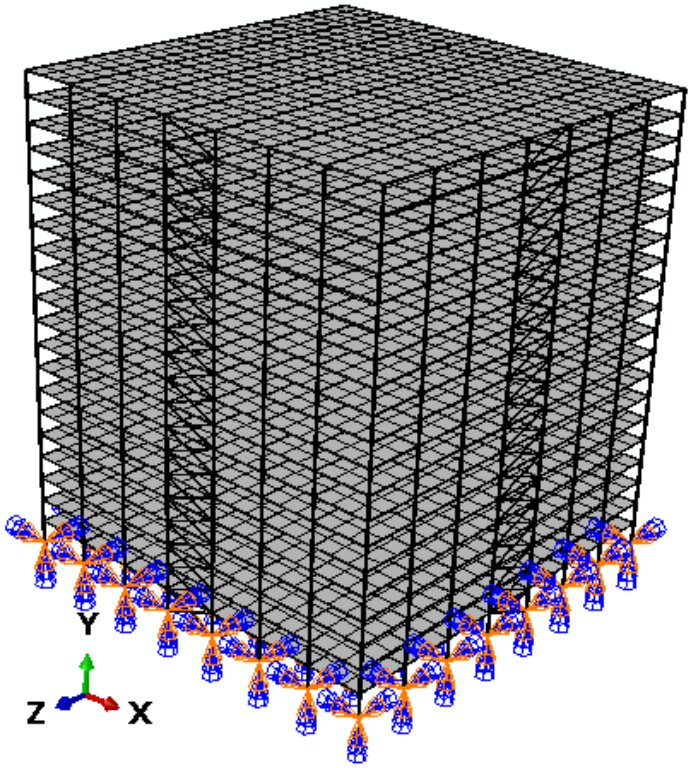

Fig. 9. FE model of 20-storey building in ABAQUS

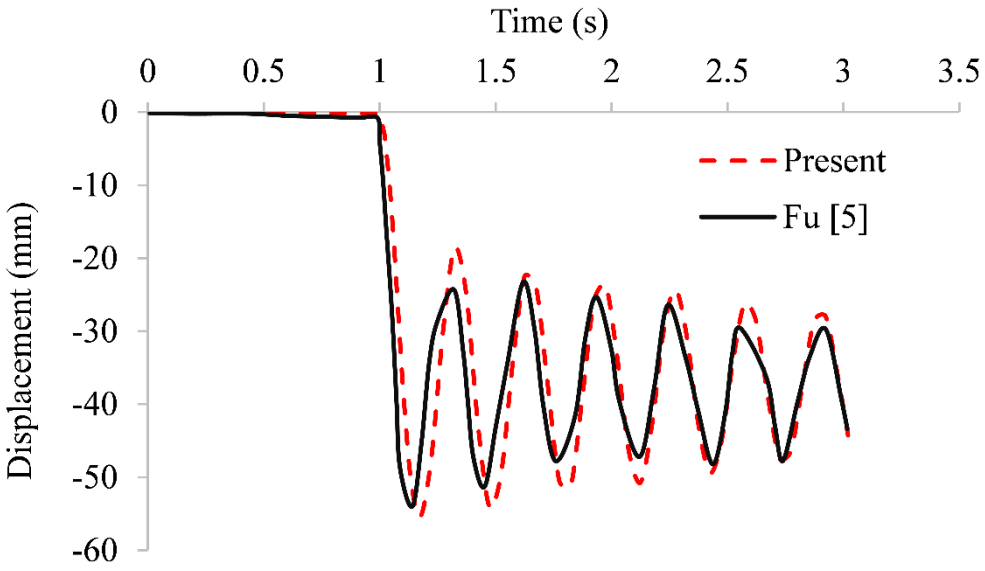

(a) Displacement-time history of the node above the removed column

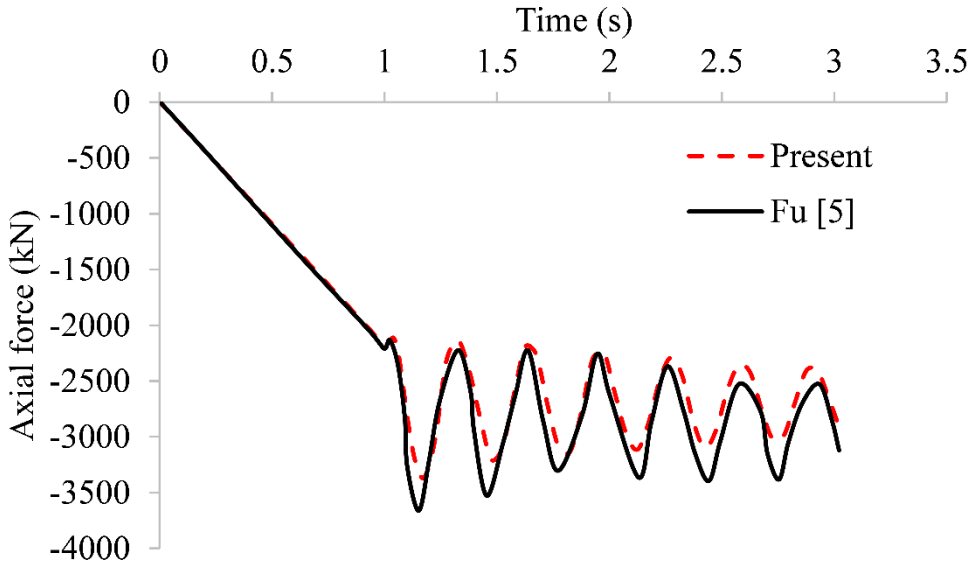

(b) Axial load-time history of the column adjacent to removed column

Fig. 10. Comparison of results for 20-storey building

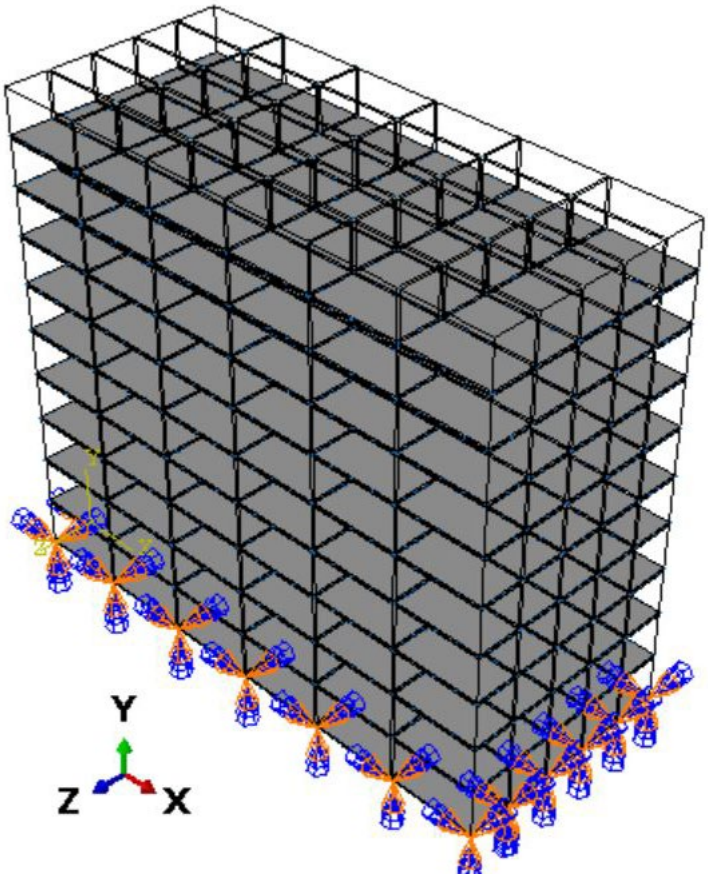

(a) 10-storey office modular building

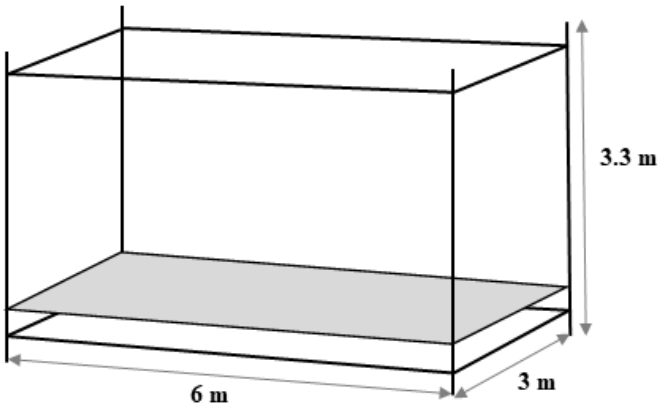

(b) Single module

Fig. 11. 3-D view of the models in ABAQUS

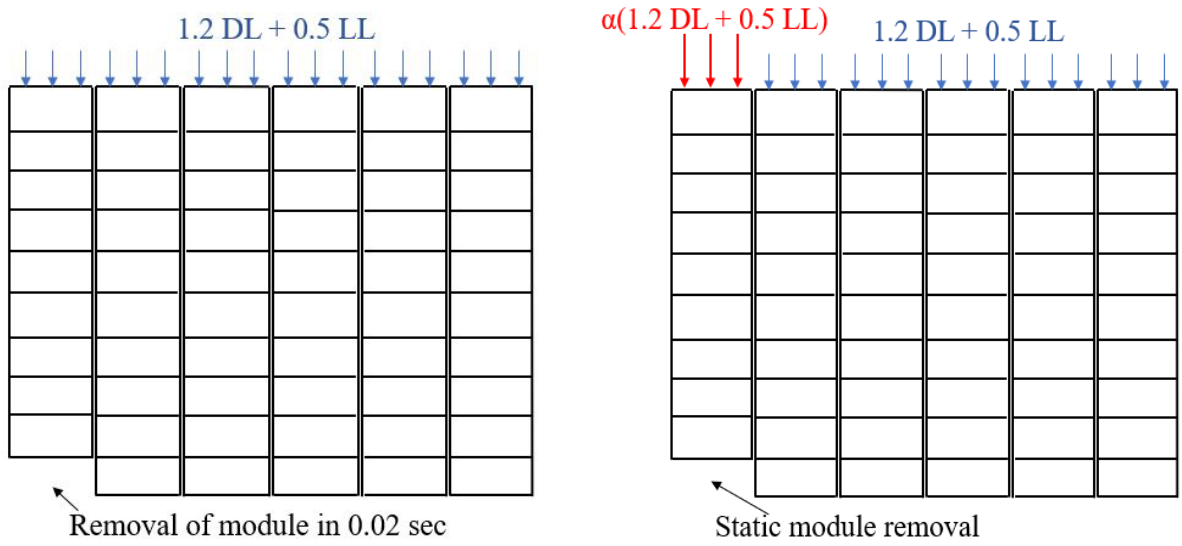

(a) Dynamic analysis (b) Static analysis

Fig. 12. Illustrations of loads

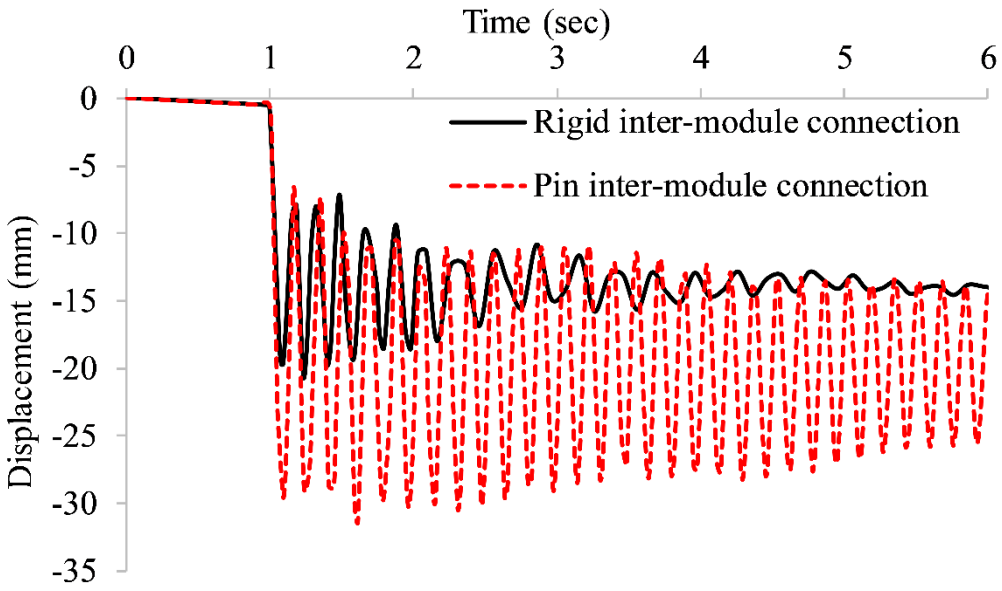

Fig. 13. Maximum displacement for 10 storey modular building with rigid and pinned inter-module connection

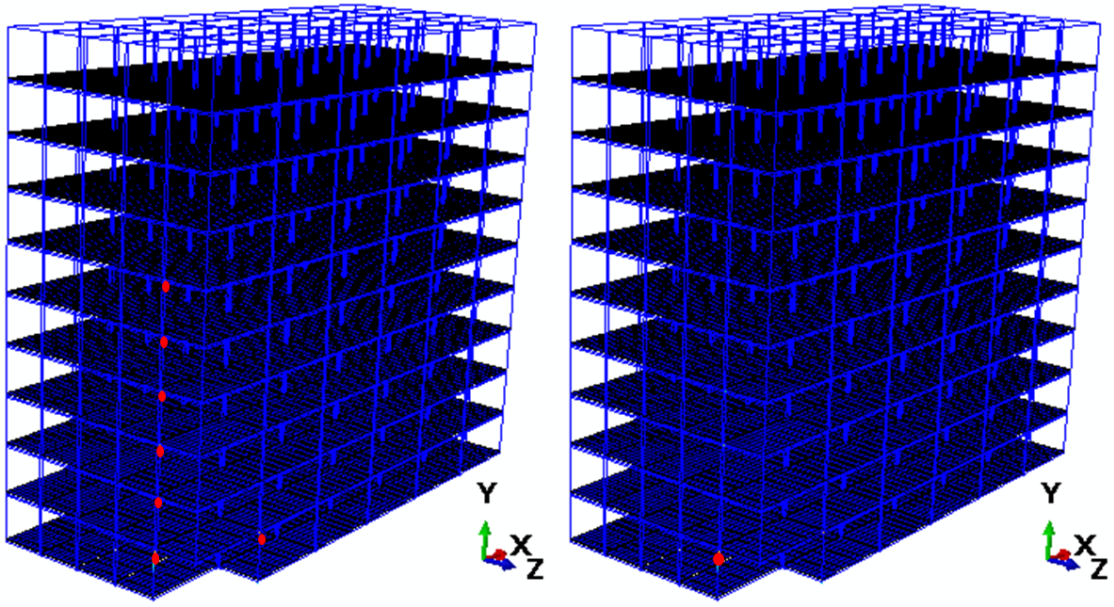

(a) Rigid inter-module connection (b) Pin inter-module connection

Fig. 14. Location of plastic hinges

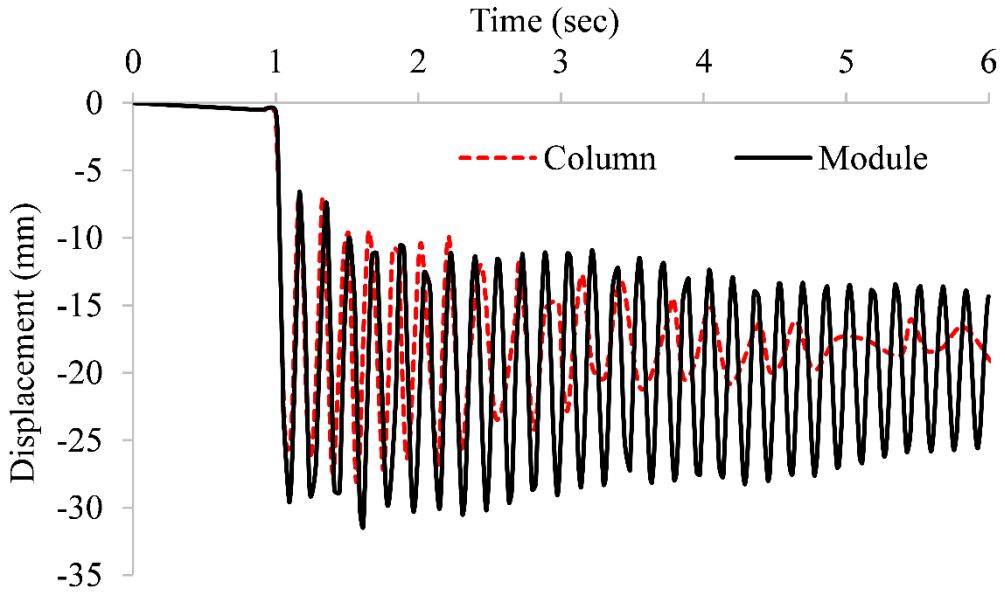

Fig. 15. Displacement time history for module and column removal scenario

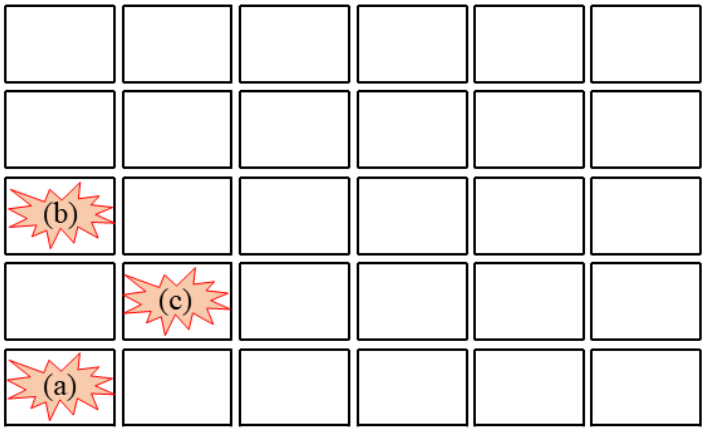

Fig. 16. Location of removed modules (a) Corner; (b) Mid span; (c) Internal

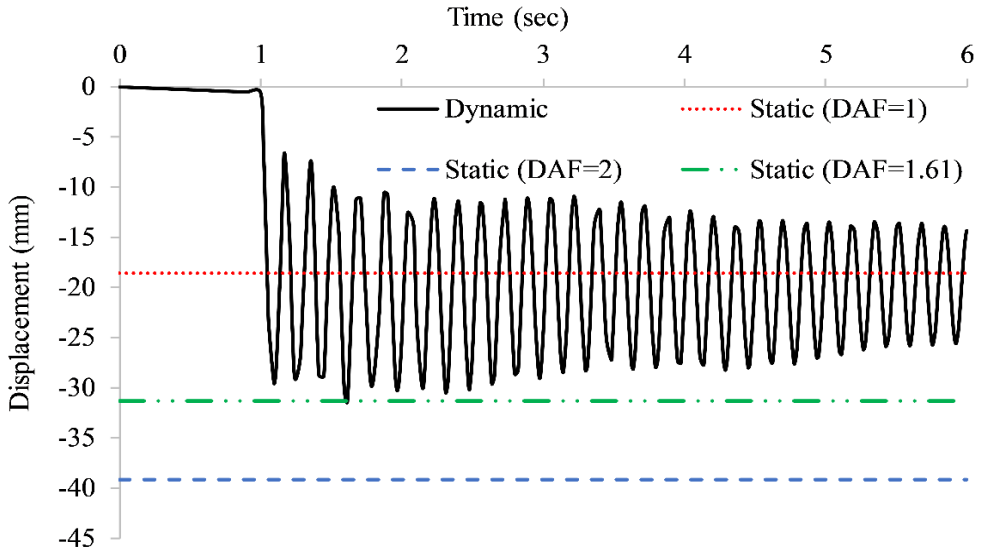

(a) Corner module removal

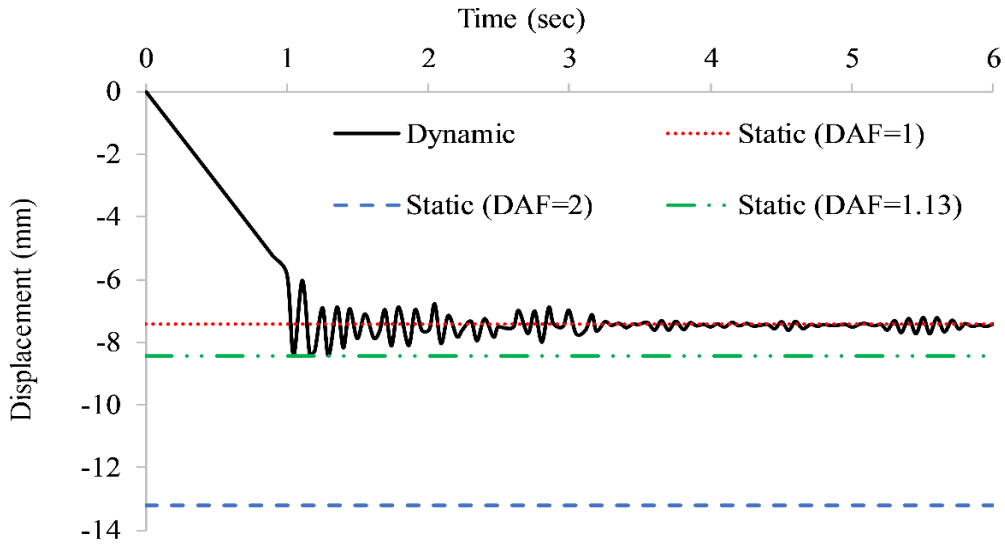

(b) Mid span module removal

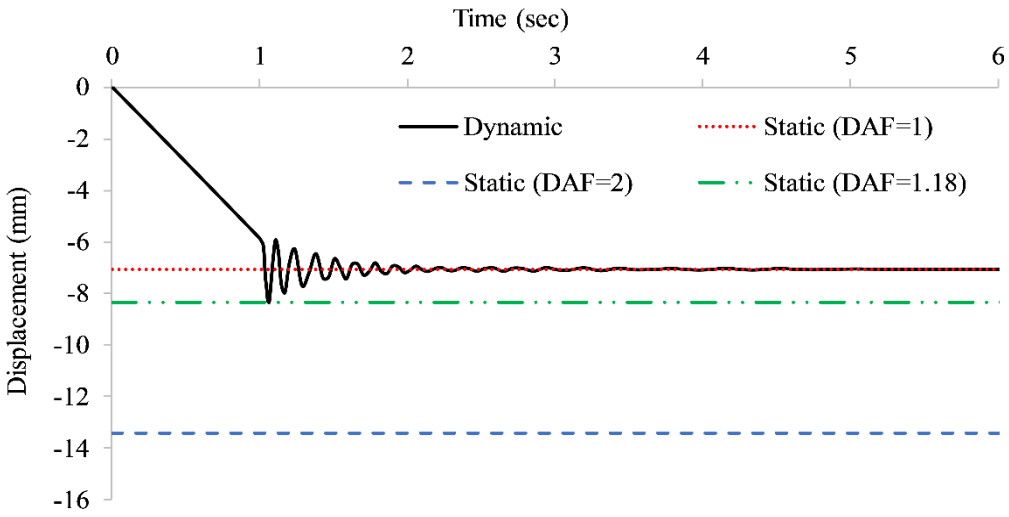

(c) Internal module removal

Fig. 17. Time displacement curve for nonlinear static and nonlinear dynamic analyses for different module removal cases

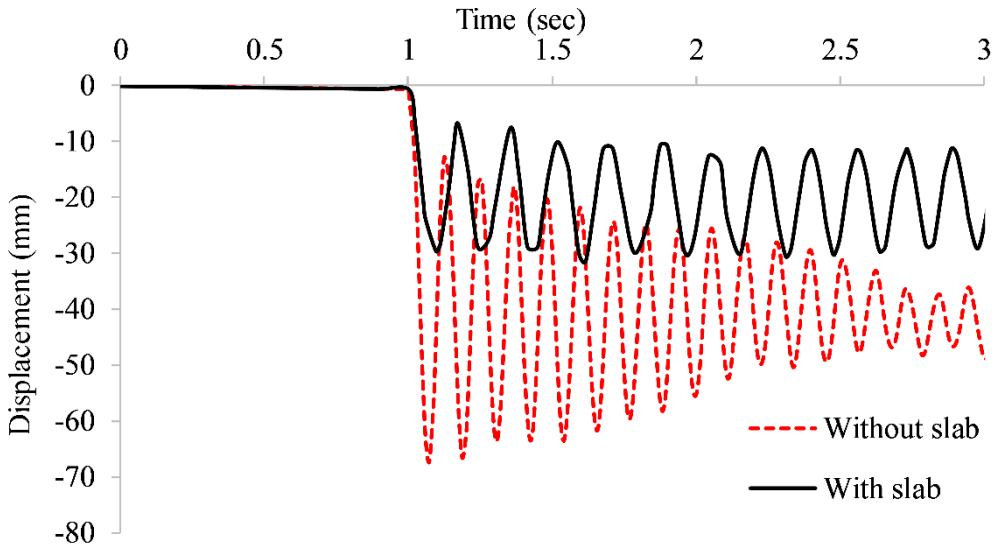

Fig. 18. Time displacement response of 10 storey modular building with and without consideration of floor slab

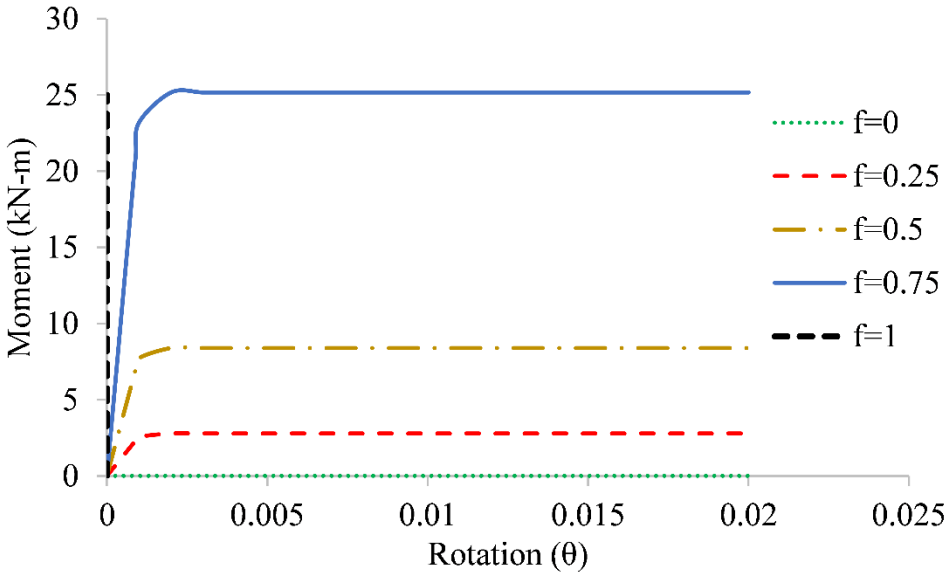

Fig. 19. Moment rotation curves for various fixity factor values of the horizontal inter-module connection

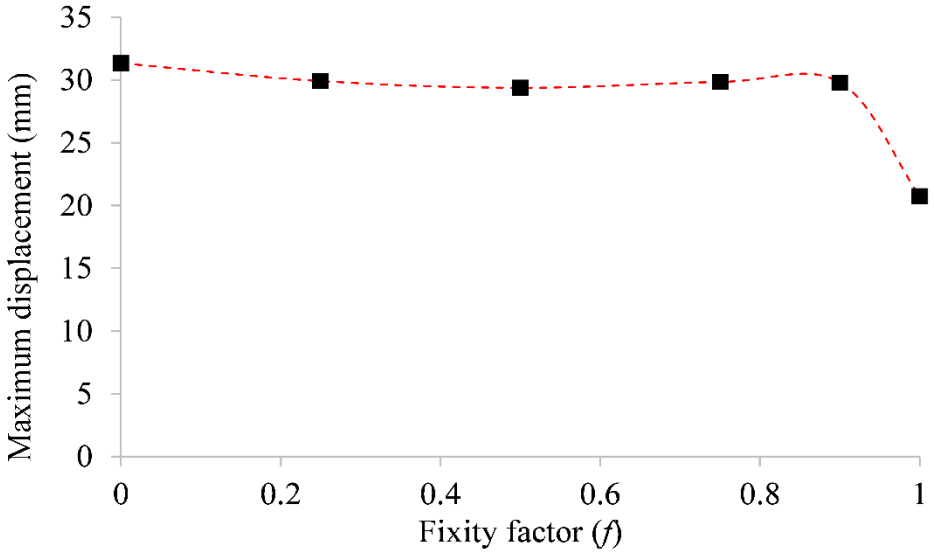

Fig. 20. Variation of maximum displacement for rigid, pin and semi-rigid connections

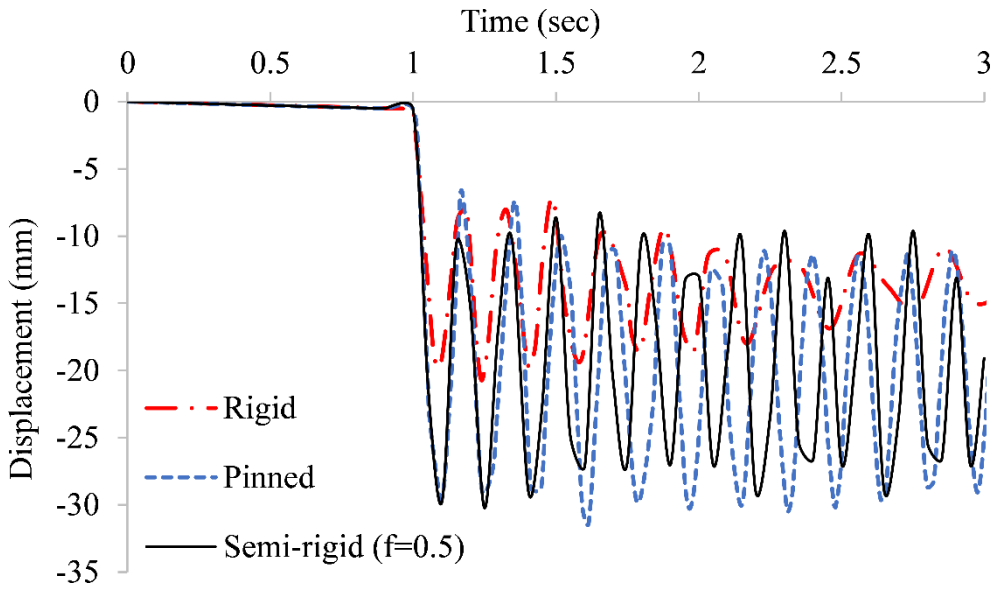

Fig. 21. Displacement time history response for rigid, pin and semi-rigid horizontal inter-module connection

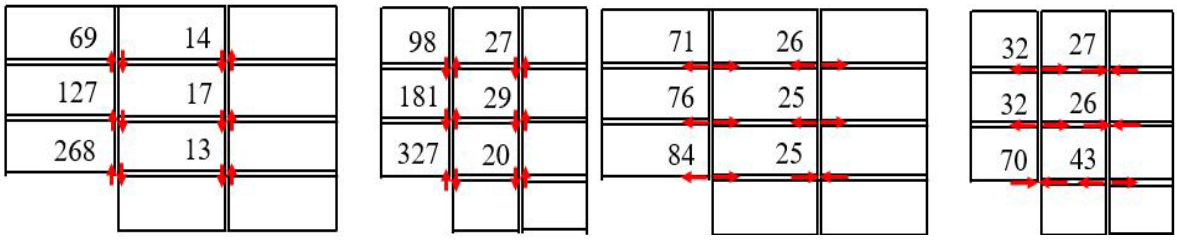

(a) Shear force (b) Axial force

Fig. 22. Horizontal inter-module connection forces for corner removal scenario in kN

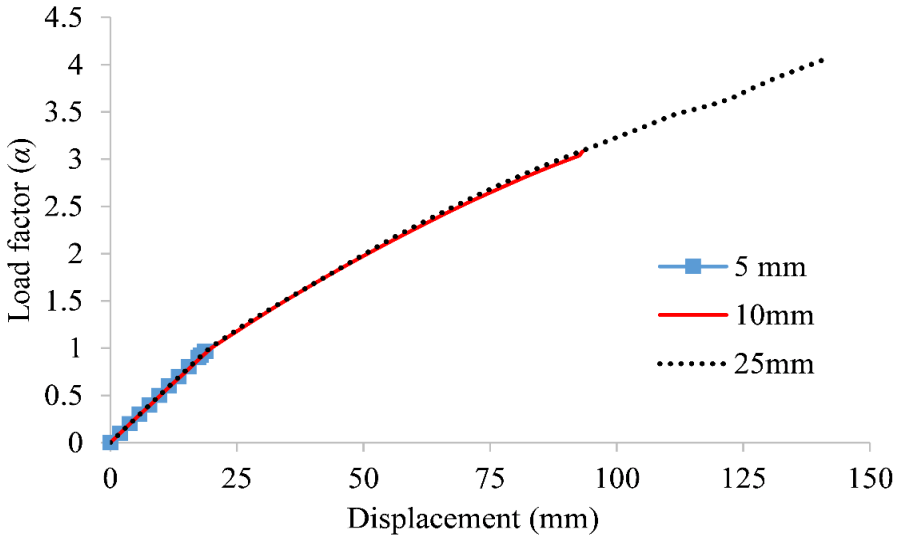

Fig. 23. Load factor vs maximum vertical displacement curve for 5 mm, 10 mm, and 25 mm horizontal gusset plate as inter-module connection

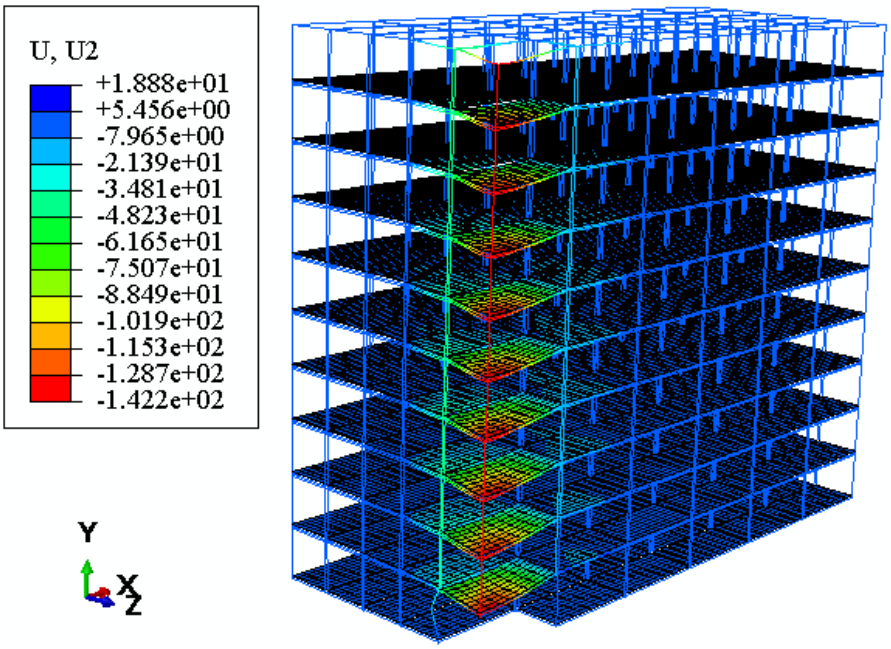

Fig. 24. Deformed shape of modular building with 25 mm gusset plate at the onset of shear failure of adjacent plate.

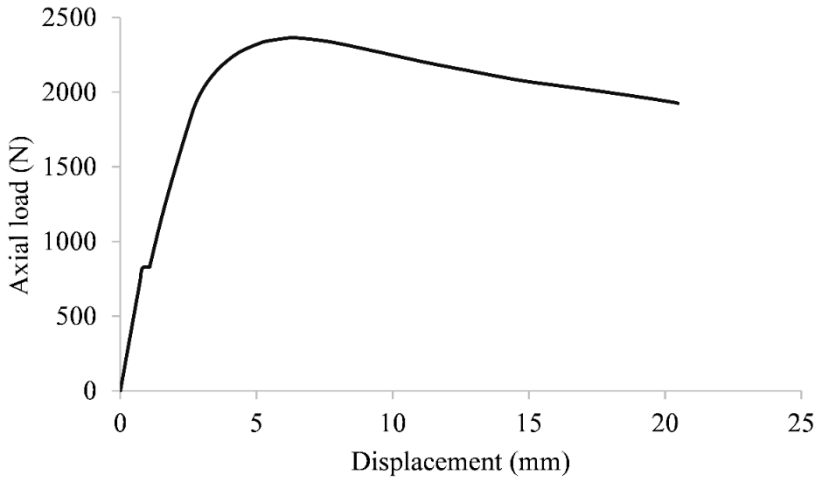

Fig. 25. Axial force vs vertical displacement curve for the adjacent column in a 25 mm plate horizontal connection.

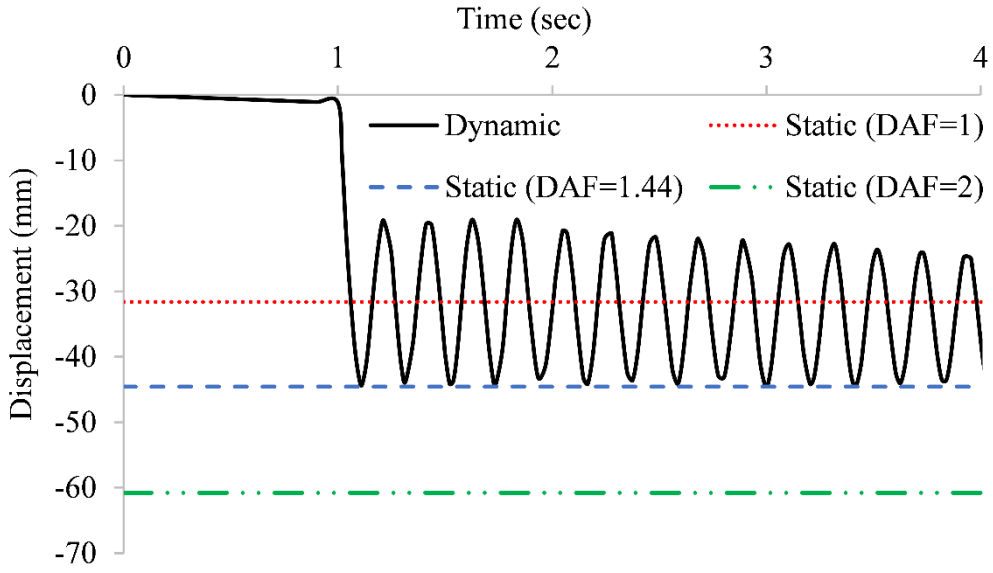

(a) 20 storey modular building

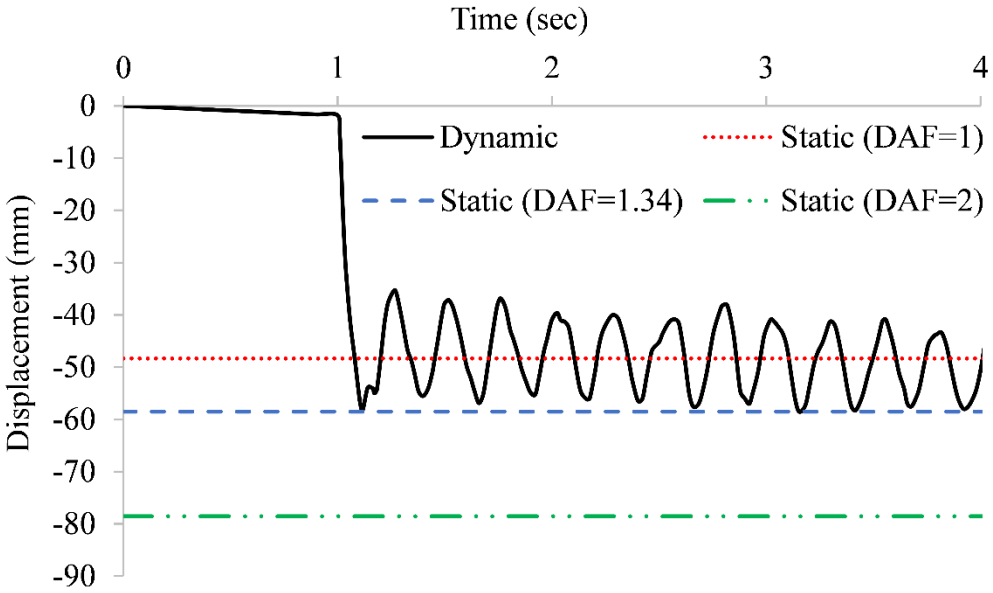

(a) 30 storey modular building

Fig. 26. Time displacement curve for nonlinear static and nonlinear dynamic analyses for corner module removal scenario